Muscle contributions to dynamic locomotion on biomimetic robots

Submitted to
Graduate School of Information Science and Technology
Osaka University

July 2014

Andre ROSENDO

Publications

Journal Papers

1. ROSENDO, A. ; NAKATSU, S. ; NARIOKA, K. ; HOSODA, K. . Producing alternating gait on uncoupled feline hindlimbs: muscular unloading rule on a biomimetic robot. Advanced Robotics, v. 28, p. 351-365, 2014.

2. ROSENDO, A. ; TANAKA, T. ; KANEKO, S. . A Yank-Based Variable Coefficient Method for a Low-Powered Semi-Active Power Assist System. Journal of Robotics and Mechatronics, v. 24, p. 291-297, 2012.

International Conferences

1. ROSENDO, A. ; LIU, X. ; NAKATSU, S. ; SHIMIZU, M ; HOSODA, K. . A combined CPG-stretch reflex on a musculoskeletal pneumatic quadruped. Intl. Conf. on living machines, LIVINGMACHINES 2014, Milan, Italy. (accepted, in press)

2. ROSENDO, A. ; NAKATSU, S. ; NARIOKA, K. ; HOSODA, K. . Pneupard: A biomimetic musculoskeletal approach for a feline-inspired quadruped robot. IEEE Intl. Conf. on Intelligent Robots and Systems, IROS 2013, p. 1452-1457, Tokyo, Japan.

3. ROSENDO, A. ; NAKATSU, S. ; NARIOKA, K. ; HOSODA, K. . Toward a stable biomimetic walking: Exploring muscle roles on a feline robot. 6th Intl. Symp. on Adaptive Motion of Animals and Machines, AMAM 2013, p. 40-41, Darmstadt, Germany.

4. NAKATSU, S. ; ROSENDO, A. ; NARIOKA, K. ; HOSODA, K. . Stable Reflex-based Walking of Forelimbs of a Bio-inspired Quadruped Robot-modeled Cheetah. IEEE Intl. Conf. on Robotics and Biomimetics, ROBIO 2013, p. 1813-1818, Shenzhen, China.

5. ROSENDO, A. ; NAKATSU, S. ; NARIOKA, K. ; HOSODA, K. . Exploring Muscular Contribution during Stepping of Biomimetic Feline Hindlimbs. IEEE Intl. Conf. on Robotics and Biomimetics, ROBIO 2013, p. 879-884, Shenzhen, China.

6. ROSENDO, A. ; NAKATSU, S. ; NARIOKA, K. ; HOSODA, K. . Exploring Stance-to-swing transition: from cats to a pneumatic quadruped robot. Intl. Workshop on Soft Robotics and Morphological Computation, SOFTROBOT2013, p. 69, Locarno, Switzerland.

7. NARIOKA, K. ; INADA, T. ; ROSENDO, A. ; SPROEWITZ, A. ; HOSODA, K. . Dynamic Locomotion of a Minimalistic Pneumatic Quadruped Robot 'Ken'. Intl. Workshop on Soft Robotics and Morphological Computation, SOFTROBOT2013, p. 82, Locarno, Switzerland.

8. ROSENDO, A. ; NARIOKA, K. ; HOSODA, K. . Muscle roles on directional change during hopping of a biomimetic feline hindlimb. IEEE Intl. Conf. on Robotics and Biomimetics, ROBIO 2012, p. 1050-1055, Guangzhou, China.

9. NARIOKA, K. ; ROSENDO, A. ; HOSODA, K. . Development of a minimalistic pneumatic quadruped robot for fast locomotion. IEEE Intl. Conf. on Robotics and Biomimetics, ROBIO 2012, p. 307-311, Guangzhou, China.

10. ROSENDO, A. ; TANAKA, T. ; KANEKO, S. . A novel semi-active assist system considering low-powered actuator limitations. IEEE Intl. Conf. on Robotics and Biomimetics, ROBIO 2010, p. 1104-1109, Tian Jin, China.

Domestic Conferences

1. NAKATSU, S. ; ROSENDO, A. ; NARIOKA, K. ; HOSODA, K. . Reflective walking of a bio-inspired quadruped robot. In: 2013 JSME Conference on Robotics and Mechanics, 2013, Saitama. ROBOMEC 2013, p. 522-525, Saitama.

2. NARIOKA, K. ; INADA, T. ; ROSENDO, A. ; HOSODA, K. . Development of a Pneumatically-driven Quadruped Robot for Fast Locomotion. JSME Conference on Robotics and Mechatronics, ROBOMEC 2013, p. 357-360, Saitama.

3. NAKATSU, S. ; ROSENDO, A. ; NARIOKA, K. ; HOSODA, K. . Development of Biomimetic Feline Robotic Forelimbs. Annual Conf. of the Robotics Society of Japan, RSJ 2013, p. 721-724, Tsukuba.

4. ROSENDO, A. ; NARIOKA, K. ; HOSODA, K. . Early Development of a Bio-inspired Feline Pneumatic Quadruped Robot. Annual Conf. of the Robotics Society of Japan, RSJ 2012, p. 212-215, Sapporo.

5. ROSENDO, A. ; HOSODA, K. . Development of a Feline Hindlimb for a Pneumatic Quadruped Robot. Special Research Comitee on Embodiment Cognitive Science and Real World Application, 2012, 10th ECSRA, p. 32-33, Tokyo.

6. ROSENDO, A. ; TANAKA, T. ; KANEKO, S. . Assist Ratio Variation Strategy for a Low-Powered Power Assist System. Japanese Robot Society - 3 Research Comittee on Robot Technology in Hokkaido, 2011, 3rd RSJ-HRT, p. 27, Sapporo.

7. ROSENDO, A. ; NAKANO, M. ; TANAKA, T. ; KANEKO, S. Design of controller for a semi-active assist mechanism considering low-powered actuator limitation. JSME Conference on Robotics and Mechatronics, ROBOMEC 2010, p. 310-314, Asahikawa.

8. ROSENDO, A. ; LEPIKSON, H. Electromyography-based power amplifier exoskeleton for human assisting purposes. Brazilian Nat. Conf. in Biomedical Engineering, COBEM 2008, p. 521, Salvador, Brazil.

Awards

1. 2nd Best poster presentation on Intl. Symp. On Adaptive Motion of Animals and Machines, AMAM2013, Darmstadt, Germany.

Thesis advisor: Professor Toru Fujiwara Andre Rosendo

Muscle contributions to dynamic locomotion on biomimetic robots

Abstract

The dream of android robots sharing human environment, widely represented in fiction books and movies, faces a few obstacles before turning into reality. Wheeled structures have been used for many years, and their low-complexity allowed wheeled robots to simplify their locomotion and concentrate in other functions. Legged locomotion, on the other hand, although older than wheeled locomotion, has only started to see developments in the last 25 years. Currently, legged robots performance is inferior even to the simplest form of natural locomotion, being vastly outperformed by animal locomotion in every aspect.

Animals transit between gaits and adapt to uneven terrain with perfection, and recent research with decerebrate animals points to the possibility of stable walking by solely using brainstem, spine and muscle signals. The innerworking of such biological locomotion is still not fully understood, where from one side biologists observational approach lacks depth on separating individual contributions, while roboticists, inspired by their locomotion, try to replicate it creating control methods which reproduce their joint angles.

In this work, the author adopts a third approach, using biomimetic robots to understand animal locomotion. Replicating the musculoskeletal structure from humans and animals allows us to better understand locomotion, probing muscular contributions to stability and overall joint coordination. Through this approach, locomotion experiments can be done in decerebrate settings, evaluating muscle responses and their contribution to walking, running and jumping.

Here, three different biomimetic robots are used to demonstrate muscular contributions on walking and hopping behaviors. Initially, the so called biarticular muscles are investigated, demonstrating the possibility of hopping direction control on the sagittal plane. Then the contribution from stretch reflexes is analyzed, showing their importance on frontal plane stabilization, bringing rolling angles back to a straight position. Finally, the author proves with biomimetic experiments the possibility of a stable alternating gait solely by the presence of stretch receptors, transitioning from stance to swing phases.

The intrinsic stability of muscles is still fairly unexplored, and such knowledge not only deepens our knowledge over animal locomotion, but also improves legged robots performance, closing the gap between robots and animals.

Contents

Listing of figures

1

Introduction

Locomotion is the most important ability for the survival of humans and animals. From carnivores to herbivores, reaching for food and fleeing from predators are primal instincts which may lack of other basic senses, but cannot be accomplished without moving. In this thesis, the author uses robots to understand the contribution of muscles on human and animal locomotion, recreating their bodies and performing experiments. Initially, the motivation to understand how we move is explained in Section 1.1, and the background on previous locomotion-related contributions is shown in Section

1.2, considering animal observation, computer simulations and robotic experiments. In Section 1.3, the problem is stated and the adopted approach to solve it is explained. Finally, in Section 1.4 the outline for this thesis is presented.

1.1 Motivation

"That's one small step for a man, a giant leap for mankind" may have been uttered by Neil Armstrong upon setting foot on the moon, but subliminally it shows the importance of locomotion, going from point A to point B, whether on foot, wheels or flying.

Wheeled locomotion can be rarely seen in biological systems, such as pangolins, stomatopods[20] and flagella[12], while legged locomotion have been used for more than 260 million years[39]. Being wheeled locomotion already explored by humans for more than five thousand years[2], irony abounds by the fact that mankind still struggles to reproduce one of the oldest locomotion methods with robots. Even primitive life forms outperform current legged robots in performance and energy efficiency.

Current robotic approach to locomotion consists of a robotic body (usually electric motors and many sensors) being controlled by a micro controller, which reads sensors and predicts joints position to satisfy stability criteria. While a robot without a micro controller is inoperative, a decerebrate animal is still capable of walking. Differently from robots, animals cascade locomotion in three different layers: brain, spinal cord and muscles, and each one has different contributions to overall locomotion.

So far, roboticists have been trying to reproduce such locomotion mostly by replicating brain, and in fewer cases spinal cord feed-forward contribution, but muscular contribution is still widely neglected. As observed by biologists, muscle spindles may play a great role providing fast feedback response from floor contact, contributing to adaptive behavior.

In this vein, to help finish the three-piece puzzle which defines animal locomotion, this work recreates animal musculoskeletal structures and analyzes, through very simple algorithms, the contribution from such structures to locomotion stability. Approaching the same locomotion problem from a new angle, the author believes that not only a wider grasp of how animals move can be obtained, but also

the benefits from compliant musculoskeletal structures can be reaped in robotics.

The future for robotics may not have robots with muscles, but understanding muscles is a condition without which highly adaptive animal behavior cannot be understood, and, as a consequence, replicated in robots. Going beyond wheeled robots and improving legged robotic locomotion will allow robots to share the same environment that we do, seamlessly participating in our society, actively being part of our lives.

1.2 Overview of the research field

From fast eye blinks to bowel movements, muscles are the main actuator option for living organisms. Although a vast range of applications are available for muscles along our bodies, this work focuses on their contributions on legged locomotion, and thus other muscle applications will be ignored.

Research on legged locomotion has two major fronts: Animal locomotion and robotic locomotion. From a biological perspective, researchers study how humans, birds and cats walk, run and jump, contracting and relaxing their muscles while keeping stability. Robots, on the other hand, aim to achieve the same kind of behavior by following algorithms, which control their actuators (usually very different than muscles) and read sensors. A new robotic branch, called biomimetic, replicates animal morphology in robots, many times including artificial muscles, with the intent of understanding biology, being a bridge between robotics and biology. Detailed references of these 3 different fields will be presented over the next chapters.

1.2.1 Biological approach

Observation of humans and animals has been one of the oldest tools to understand locomotion. For over 100 years[7,46], biologists hypothesize the reasons why we move our body forward and what role the brain plays over such phenomenon. With advancing technology, locomotion observation included electromyography, electroencephalogram, three-dimensional motion capture and slow-motion video recording, widening our understanding on how things work.

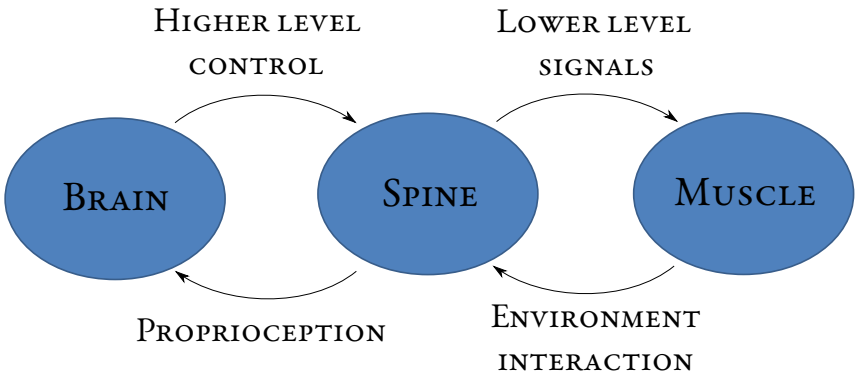

Figure 1.1: The interaction between brain, spine and muscle happens through brain signals being passed to actuators through the spine, which not only filters these signals, but is also capable of creating their own. The muscles also act as sensors, informing spine and brain of their interaction with environment, forces and joint positions.

Hitherto, experiments with animals have hinted that locomotion is a combination of three elements (as shown in Fig. 1.1), namely:

- Brain - Also called higher control, is responsible for the decision-making process. This control level receives direct input from vestibular (brainstem) and ocular system, being highly effective on keeping balanced posture, planning leg trajectory and avoiding obstacles/disturbances.
- Spinal cord - The spine, located between brain and muscles, conveys brain messages to the muscle, but is also capable of creating their own signals. Recent researches have found that the spine is a central pattern generator (CPG), creating rhythmic patterned outputs to control our muscles.
- Muscles - The last link of the chain, muscles act as actuators and sensors at the same time. Proprioception (one's idea of their own joint positions) can be achieved by signals sent from muscles to brain, but other phenomena, such as stretch reflex, may take place between muscle and spine, producing shorter delay. Their compliant behavior permits the production of force while being highly deformed, which is rarely seen in current robotics.

The image of a central entity commanding the entire body seems reasonable and easier to grasp than a multi-layered controlling method. Research with decerebrate animals has shown, however, that

locomotion is still possible without brain, proving that locomotion is broken down in different levels, allowing the brain to concentrate in more important tasks. While walking to work, a businessman might think about market strategies and lunch while, almost as if on auto-pilot, his body deals with the highly uneven floor, passing through small obstacles.

The interaction between brain, spine and muscle happens through higher level commands being sent by the brain to the spine, consisting of an intended movement. The spine, upon receiving such commands, adapts this higher request to the lower level architecture, overdriving, amplifying or changing the lower level rhythmic motion before passing it down to muscles. The muscles, on the other hand, sense their deformation upon touching the floor, communicating directly to the spine to reach faster responses and adapt to disturbances, unexpected by both brain and spine.

1.2.2 Robotic approach

Upon watching how animals move, scientists decided that such adaptive locomotion could also be used on robots, taking them through places where wheeled robots could never pass through. However, animal joint movements are produced by muscles, and their high compliance combined with non-linear behavior makes it difficult to reproduce the same intended movement on a robotic actuator. Thus, roboticists' take on legged locomotion adopts legs as end effectors of a manipulator, using motion equations to estimate the optimal trajectory to keep the body upward while moving. This approach, defined by Wisse[67] as static bipeds, is "a good starting point for industrial developers", not being, however, source of explanation of how animals do it.

Through this approach, which keeps the center of mass above the foot contact area, robot controllability can be achieved by estimating all joint positions related to the floor. Similarly to industrial manipulators, leg trajectory is calculated and strictly followed, and disturbances should be accounted through sensors (vision, distance, and so on). Approaches such as Zero Moment Point[66] are extensions of this method, keeping the center of pressure inside the foot contact. Although more dynamic than initial methods, these methods are still highly static, producing unnatural gaits, incapable of adapting

well to unforeseen ground disturbances.

In 1990, McGeer[37] introduced a novel approach to legged robotics, showing that stable walks could also be performed by unactuated legged robots. The so called Passive Walkers were capable of walking down a stable slope, exploiting gravity to produce leg swinging. Not only being extremely energy efficient, the proposed walking method also produced a fairly natural gait when compared to other existing stable robotic gaits. A few years later, van de Linde[62] explored the same idea to produce robots capable of walking in flat surfaces, replacing the gravity contribution by active springs (pneumatic artificial muscles, or PAM for short). The gait naturality in this method is extremely close to human walking, leading us to believe that the inner workings of animal walking can be replicated and understood with such approach.

1.3 Problem Statement and Approach

Although improved with technology, biological observation is still limited by the biological organism itself. To fully grasp how animals move, and their inner workings, reproducing their movements from a muscular level is a necessary step. Similarly to an infant learning how to walk, as important as observation might be, the only way to understand it is by trial and error.

In the last few years, Pfeifer suggested that the interaction between body and environment was extremely important, being locomotion an emerging phenomenon from such interface[45]. Thus, with body shaping our minds and not the other way around, understanding our ignored musculoskeletal system might close the gap between animals and robots.

The approach adopted on this work uses pneumatic artificial muscles (similarly to those used by van de Linde[62]) to recreate musculoskeletal structures of animals, with similar muscles and link lengths. Adopting simple algorithms to control muscle contractions and simulate neurophysiological rules, this work evaluates contributions from muscles to locomotion, initially with simpler cases like hopping and, later, walking. Since different morphologies excel in different tasks (leopards, cheetahs and lions hunt in different ways), each experiment used a different leg morphology, pinpointing locomotive

attributes from different animals.

Although closely resembling animals, many differences still exist between real animals and the adopted biomimetic robots. Hoping to push forward the boundaries of biological knowledge, the author hopes that future biological experiments support the ideas herein proven. Nonetheless, experiments were performed focusing on the hypothesis to be proved and trying to minimize effects which could occur from design differences.

1.4 Thesis Outline

In this work, three different biomimetic robots are used to explain phenomena observed within muscles of humans and animals. In Chapter 2 a biomimetic hindlimb from a cheetah (similar link lengths and muscular arrangement) is used, and the contribution from biarticular muscles to sagittal hopping stability is analyzed. This hopping hindlimb experiment was the initial study of what became the "Pneupard project", aiming to better understand the fast locomotion of felines. As an outcome, a better understanding of biarticular muscles on limbs was achieved, exploring the muscle semitendinosus as an active spring, controlling hopping direction with different pressure values.

While experiments from Chapter 2 with feline hindlimbs explored sagittal plane movements, in Chapter 3 a humanoid robot is used for frontal plane hopping. It is hypothesized that, upon landing in a tilted posture (one leg touching the floor before the other), the presence of muscular stretch reflex brings the system to stability, not requiring attitude information. Experiments showed that this hypothesis is true, and introducing a delay between touching the floor and the reflex response did not degrade this phenomenon, indicating that muscles play an important role on bipedal stability.

With muscle contributions on hopping from frontal and sagittal planes investigated, walking was chosen as the next studying step. In Chapter 4, a pair of robotic feline hindlimbs (Pneupard project) are attached to a slider and a finite state machine forces these two limbs to transit between stance and swing phase, independently. In recent biological experiments it was hypothesized that the transition from stance to swing is controlled by the reduction of load on the ankle extensor, exciting the flexor

muscles to swing forward. During experiments it was proven that, although completely uncoupled, right and left hindlimbs alternate themselves as a consequence of stretch receptor signals.

Finally, in the last chapter, possible contributions to biology and robotics are considered. The applications of legged robots and the usage of muscles in such robots are discussed, concluding this work.

This chapter is largely based on the article:

Rosendo A, Narioka K, Hosoda K. "Muscle roles on directional change during hopping of a biomimetic feline hindlimb", Proc. IEEE ROBIO 2012, Guangzhou, pp. 1050-1055[16].

2

Muscle roles on sagittal plane hopping

Cats, from tiny domestic cats (*Felis catus*) to big tigers (*Panthera tigris*), are well known for their great acrobatic skills and hunting ability. Aiming to better understand how the feline family interacts with the environment, we adopt a biomimetic approach on a hopping feline hindlimb. Using air muscles to simulate the compliance of biological muscles, this robotic hindlimb has seven muscles and changes hopping direction. We individually evaluate and estimate muscles contribution to the jumping direction. Finally, we successfully control the hopping direction using a non-linear curve fitting from experimental results, hopefully contributing to the understanding of our biological counterpart.

2.1 Introduction

Members from the *Felidae* family have always amazed researchers for being the pinnacle of landed animal's locomotion. Abilities such as tree climbing, soft landing and high speed locomotion are some of their feats which baffle biologists and robotic researchers. For more than 100 years, researchers have been trying to pinpoint the secret for such intriguing proficiency, but due to highly complex and redundant muscular structures, this biological conundrum, so far, have not been fully explained or mimicked.

With the advent of electromyographic (EMG) sensors, improved image capturing and digital computers, biologists could deepen their knowledge on musculoskeletal behavior of animals. Great works that could be mentioned would be Engberg and Lundberg[15], Goslow[23,51], and English[16].These works used EMG and biometric data to understand muscular activation pattern within the feline gait, reaching the conclusion that quadruped step cycle is divided in four phases and, independent of gait pattern or speed, is controlled by 3 muscular patterns.

Although these works helped understanding overall feline musculoskeletal behavior, particular muscular function (*i.e.* isolated from the redundancy of dozens of muscles *in vivo*) was still very hard to understand. Light started to be shed on this problem with the approach of mechanical energy transfer done by the so called biarticular muscles[49,50], which has as its foremost researcher van Ingen Schenau (*e.g.*,[63] and[22]). These muscles were proven to contribute to energy transfer between proximal and distal joints, keeping coordination between joints, thus helping on the final direction of the external force[27].

Drawing inspiration from biological systems, roboticists have been trying to mimic animal locomotion for some time. Considering geometrical resemblance we could mention Tekken 2 and Oncilla, which are controlled by electrical motors and have a passive element at each leg to soften the contact with the floor[19,59]. Although these robots have remarkable performance, with stable locomotion along different gait patterns, their robotic actuation system differs drastically from biological systems.

Due to this fundamental difference, the development of a robotic hindlimb which faithfully represents the biological system should possess some degree of actuation and compliance in every joint, as observed in muscles. In this aspect a few robots could be mentioned, such as Puppy[3], which is a canine robot driven by pneumatic muscles, capable of drawing power while being elastic, similarly to the pneumatic robot created by Tsujita[60]. Another example would be the Cheetah robot[34], which combines electric motor and pneumatic cylinder inside the same muscle, possessing a simplified structure of only 2 muscles per leg. Also worth citing is the robot Kenken[30], which had a spring simulating the behavior of the muscle gastrocnemius. Although closer to a biological representation, these four robots had over-simplified muscular structure, not allowing mono and biarticular role studies.

To the best of the authors knowledge, works that better represented artificially this biological complexity, including mono and biarticular muscles, were the works of Ekeberg[14], Niiyama[41] and Hosoda[27]. While Hosoda and Niiyama focused on human locomotion during jumping and running, with Hosoda investigating specifically biarticular muscle roles during jumping, Ekeberg developed a feline walking computer simulation, capable of adapting to terrain irregularities.

In this paper, we attack the animal locomotion problem with a more biologically faithful approach. Adopting a hindlimb structure similar to the one explored by Ekeberg, we evaluated the contribution of mono and biarticular muscles during directional change of a feline jump while attached to a slider.

The robotic hindlimb is tested during hopping with different settings for gastrocnemius, semitendinosus and iliopsoas, and their contribution to the landing position is evaluated. Our hindlimb is capable of changing hopping direction by changing the level of air pressure at the semitendinosus muscle, being controlled by a non-linear relationship. In the future, this same method will be applied to a full body robot, inducing controlled bounding and pronking behaviors, hopefully solving remaining questions on animal locomotion.

Table 2.1: Pneupard's hindlimb key characteristics

Property	Value
Thigh length	287 mm
Shank length	345 mm
Foot length	132 mm
Body weight	870 grams
Hindlimb weight	450 grams
Total weight	1.32 kg

2.2 Materials and Methods

In order to better understand the feline hindlimb, and later apply this muscular knowledge to any other animal, we believe that a constructivist approach is needed. Instead of observing the muscular behavior of a cat and trying to speculate how dozens of muscles are correlated, we believe that artificially replicating the same morphology and inducing the contraction of the muscles under investigation can produce more fruitful results, as discussed in [27].

For this research, due to physical constraints from air muscles (short muscles are unfeasible), a hindlimb of a sufficiently big cat had to be chosen. Considering its jumping proficiency, we adopted as biological model a *Panthera Pardus*, which will be integrated in the future with a full body pneumatic robot, hence named Pneupard. The specifications for the hindlimb can be found on table 2.1, while the picture of the same attached to the slider on Fig. 2.1.

The attachment between the hindlimb and slider allows body rotation over sagittal plane, where this rotation axis is aligned with the hip rotation axis. Due to the non-existence of digits, the hindlimb touches the floor with the tip of its metatarsal link (foot).

Similarly to the computational model adopted by Ekeberg[14], the adopted hindlimb possesses 7 muscles, with 5 monoarticular muscles performing ankle flexion (tibialis anterior, TA), ankle extension

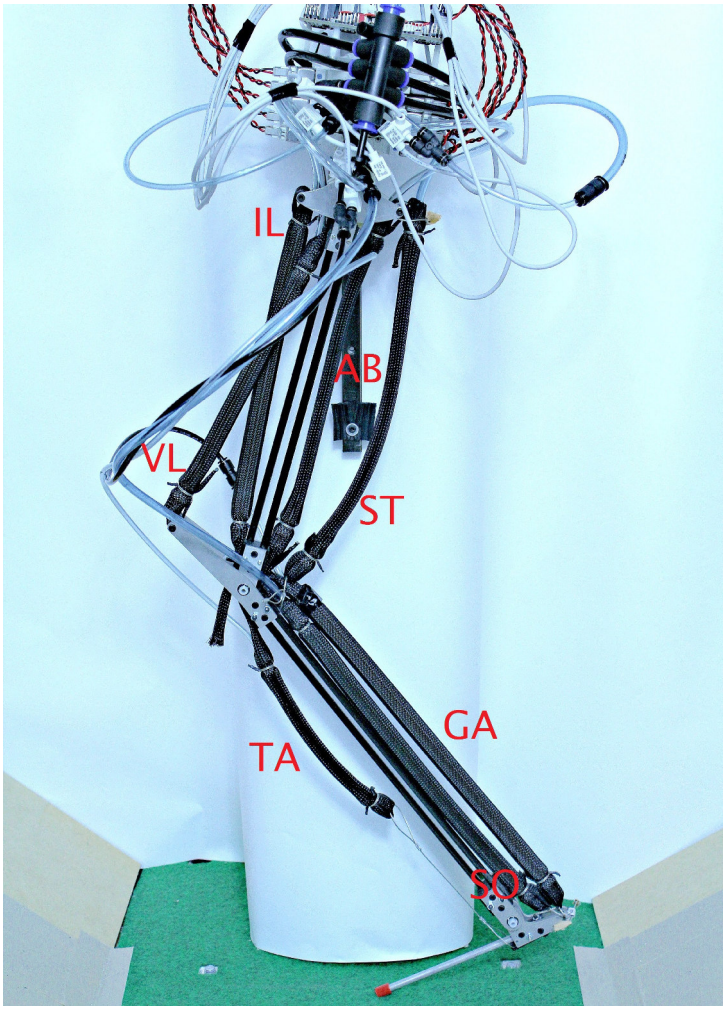

Figure 2.1: Feline hindlimb attached to slider. Vertical translation and sagittal rotation are possible between the hip and the slider.

(soleus, SO), knee (stifle) extension (vastus lateralis, VL), hip flexion (iliopsoas, IP) and hip extension (anterior biceps, AB), and 2 biarticular muscles performing knee flexion and ankle extension (gastrocnemius, GA) and knee flexion and hip extension (semitendinosus, ST).

2.2.1 Air muscle consideration

While animals possess biological muscles, which provide actuation combined with compliance to interact with the environment, the same so far is not available for human-created structures. Alternatives

such as series elastic actuators [48] came into play for almost 20 years, but the amount of weight added to the robot is cumbersome. When it comes to power-to-weight ratio, actuators such as air muscles outperform any other alternative, reaching ratios as high as 400:1, being successfully used in robotic applications [27].

The principle of activation is based on the intake of air through a pneumatic valve, which generates a contraction of the muscle, while exhausting the same air relaxes the muscle. The compliance offered by the actuator is proportional to the muscle contraction, while the force provided by the same is, as mentioned in [6], dependent on the internal pressure and muscle deformation, as shown in the following equation:

$$F \propto \frac{p_{air}}{\Delta l / L_0}$$

where F is the force, p_{air} is the internal pressure, L_0 is the relaxed length and Δl is the deformation after muscular activation. Comparisons have shown that although force-length properties of these actuators are muscle-like, with higher activation pressures resulting higher forces and longer muscles generating higher outputs than short ones, force does not decrease with increasing contraction speeds [31]. To be considered as a fair replacement it should be used below the resting length (biological muscles degrade performance above this length) and at low contraction speeds, as used during walking experiments. The resemblance between these artificial muscles and biological ones have been exploited by roboticists [68] and biologists [4].

These actuators are made from a rubber tube with 8 mm internal diameter and 1 mm thickness, covered by a polyester exterior braid with minimum diameter of 9 mm and clamped in both sides with plastic connectors with 8 mm diameter, where a cap seals one side and a plastic tube provides air through the other. The construction process is fairly easy, allowing the use of different lengths to find the best performance. Thus, such muscles were used in all three different robots demonstrated in this thesis.

2.2.2 Muscular Activation and Pattern

The muscular activation is done by pilot-operated on-off pneumatic valves. Instead of a "bang-bang" approach for muscular contraction, we opted for a hysteresis control approach, being capable of controlling the air pressure inside each muscle. The maximum pressure used for jumping was 0.6 MPa, and the aforementioned control method allows incremental pressure changes of 0.01 MPa.

The hindlimb is controlled through a micro controller, attached to its body and connected to a computer. The micro controller, called Adaptive Board and created by our Adaptive Robotics Laboratory, runs an ARM 76 MHz processor and samples data from the hindlimb at a frequency of 1 kHz, transmitting to the computer at a frequency of 40 Hz. A tether connected to the hindlimb allows communication, along with supplying energy and compressed air.

The hopping pattern adopted for Pneupard's hindlimb is largely based on the jumping pattern demonstrated in [27], but with crucial differences: Since this work focus on a feline hindlimb, a digitigrade stance is possible by a higher torque on the ankle, while Hosoda's work focused on a plantigrade human morphology. Moreover, our robot starts jumping from the ground, instead of falling from a higher position.

From the initial position we control the muscles GA, ST and IL to reach a desired pressure. When these 3 parameters are fixed, the hindlimb jumps by supplying air to SO, AB and VL, which are the three main extensors, until the leg loses contact with the floor, where the muscle AB is relaxed (exhausted) and IL contracts even more. All monoarticular muscles are relaxed when the apex is reached (close to 250 ms) to prepare for landing, where only the biarticular muscles absorb the impact. After impact, IL is once again regulated to reach the controlled value. A schematic demonstrating this activation pattern is shown in Fig. 4.5.

2.2.3 Role of Biarticular Muscles

To understand the role of biarticular muscles, we elaborate an explanation from [22]. Similarly to van Ingen Schenau, we can depict the body acting against an external force, such as the ground reaction

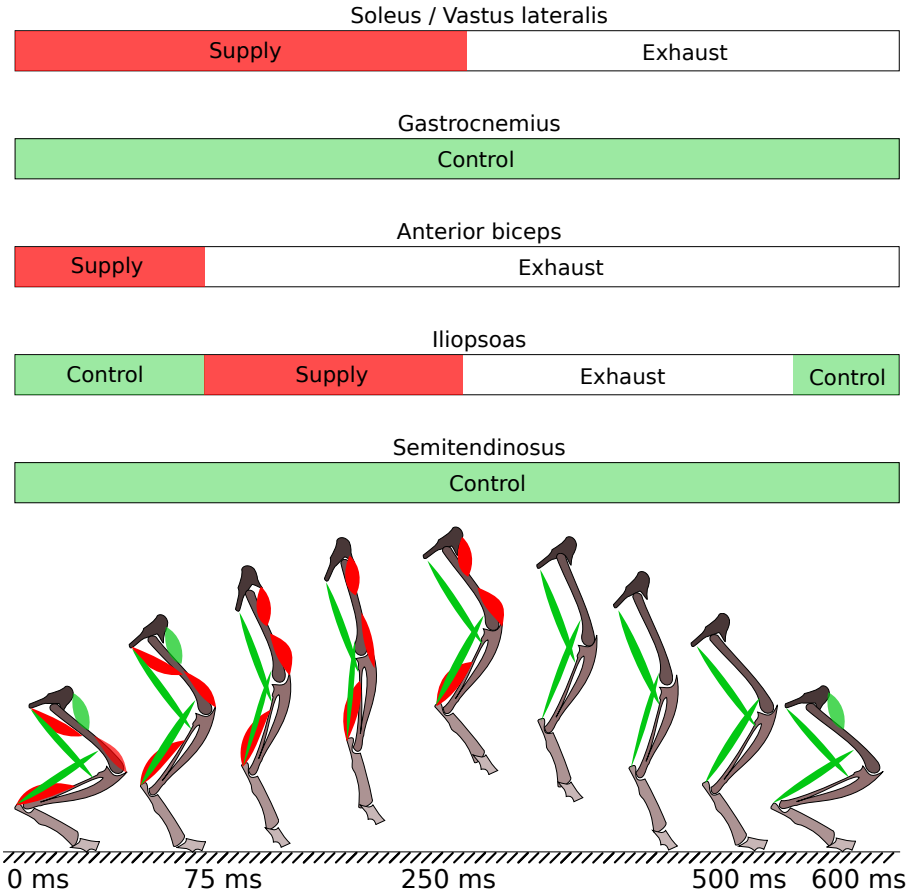

Figure 2.2: Activation pattern of hindlimb, starting from ground position, reaching apex and landing.

force (GRF) during landing in Fig. 2.3.

Notice that the total work done by the tip of the foot is the sum of works done by the other joints:

$$\Delta W = T_{hip}\Delta\vartheta_{hip} + T_{knee}\Delta\vartheta_{knee} + T_{ankle}\Delta\vartheta_{ankle} \tag{2.1}$$

Considering the frame of reference at the hip (Fig. 2.3B), the cartesian position of the foot would be defined as:

$$\begin{matrix} x \\ y \end{matrix} = \begin{matrix} -l_{thigh}cos(\vartheta_{hip}) - l_{shank}cos(\vartheta_{hip} - \vartheta_{knee}) - l_{foot}cos(\vartheta_{hip} - \vartheta_{knee} + \vartheta_{ankle}) \\ -l_{thigh}sin(\vartheta_{hip}) - l_{shank}sin(\vartheta_{hip} - \vartheta_{knee}) - l_{foot}sin(\vartheta_{hip} - \vartheta_{knee} + \vartheta_{ankle}) \end{matrix} \tag{2.2}$$

and for small displacements the relation between the changes in joint angles with changes at the tip of the foot would be:

$$\begin{bmatrix} \Delta x \\ \Delta y \end{bmatrix} = J \begin{bmatrix} \Delta \vartheta_{hip} \\ \Delta \vartheta_{knee} \\ \Delta \vartheta_{ankle} \end{bmatrix} \tag{2.3}$$

where J is the Jacobian, given by:

$$J = \begin{bmatrix} l_{thigh}sin(\vartheta_h) + l_{shank}sin(\vartheta_h - \vartheta_k) + l_{foot}cos(\vartheta_h - \vartheta_k + \vartheta_a) \\ -l_{thigh}cos(\vartheta_h) - l_{shank}cos(\vartheta_h - \vartheta_k) - l_{foot}cos(\vartheta_h - \vartheta_k + \vartheta_a) \\ -l_{shank}sin(\vartheta_h - \vartheta_k) - l_{foot}sin(\vartheta_h - \vartheta_k + \vartheta_a) \quad l_{foot}sin(\vartheta_h - \vartheta_k + \vartheta_a) \\ l_{shank}cos(\vartheta_h - \vartheta_k) + l_{foot}cos(\vartheta_h - \vartheta_k + \vartheta_a) \quad -l_{foot}cos(\vartheta_h - \vartheta_k + \vartheta_a) \end{bmatrix} \tag{2.4}$$

Finally, the relationship between a change in the external force and a change in joint torques would be:

$$\Delta T = J^T \Delta F \tag{2.5}$$

Considering T_{ankle} as a reaction to GRF generated by ankle extensors, activating biarticular muscles would be more effective than relying on monoarticulars. The reason for this comes from the tapered muscular structure that mammals usually possess, where power (muscle) is concentrated on proximal members, connecting to distal members with fewer muscles or tendon/sheath structures, such as the human hand. Transferring energy from the strong knee extensor VL through GA reduces the force needed on SO (as demonstrated in Fig 2.3B). The relationship between SO and GA was quantitatively approached in [49].

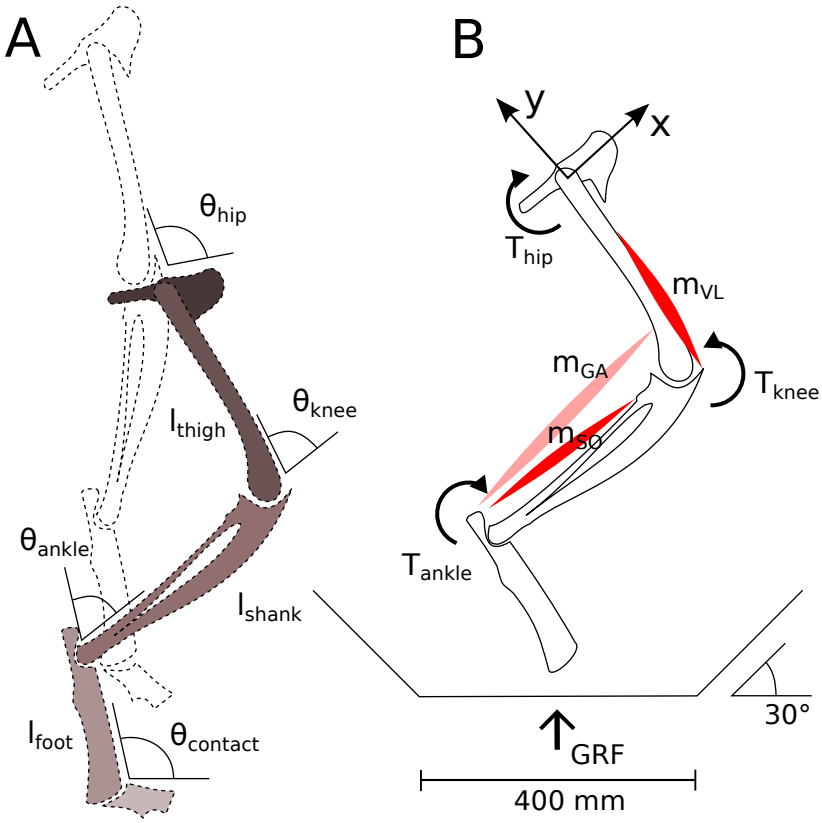

Figure 2.3: Role of biarticular muscles, demonstrating relationship between GA, SO and VL.

2.2.4 Experimental Procedure

We performed experiments by attaching the hindlimb on a linear slider, allowing the body to rotate along the sagittal plane. Due to horizontal translational constraints we added two slopes, each one 200 mm away from the slider's vertical projection, elevating 30 degrees to allow foot contact at steeper angles, as seen in Fig 2.3B.

At the first phase of the experiment the pressure at IL, GA and ST was fixed at a determined value and the hindlimb hopped 25 times. The landing position of each jump was recorded and new parameters for IL, GA and ST were set. Instead of recording the landing position with angular information, we judged that adopting distance would be more precise, since the hindlimb's height is specially affected by the pressure at GA.

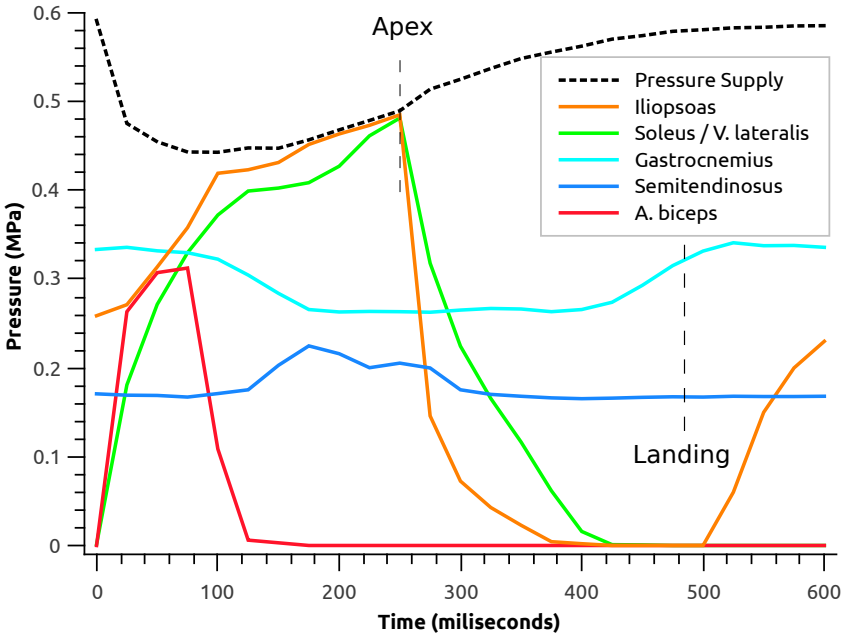

Figure 2.4: Muscular activation (pressure) during hopping on a plane. The pressures of 5 different muscles are depicted along with the supply pressure.

For the second phase of our experiment we used data acquired from the first phase and controlled a hopping hindlimb, following a target value during 72 sequential jumps.

2.3 Results

Initial data acquired from hopping shows the behavior of muscles during one hopping. Pressure inside of each muscle was recorded at a sampling rate of 40Hz, where the hindlimb takes off, reaches apex and lands, preparing for the next jump, as seen in Fig. 2.4. Pressure at GA, ST and IL were 0.33, 0.18 and 0.25 MPa, respectively.

Systematically tuning pressure values for IL and ST, both responsible for rotating the hip, and averaging the results of 25 sequential jumps for each configuration, we plotted a tridimensional graph, as seen in Fig. 2.5. The adopted pressure for GA at these tests was 0.33 MPa. Any landing position above 200 mm or below -200 mm should be understood as the limb climbing the slopes.

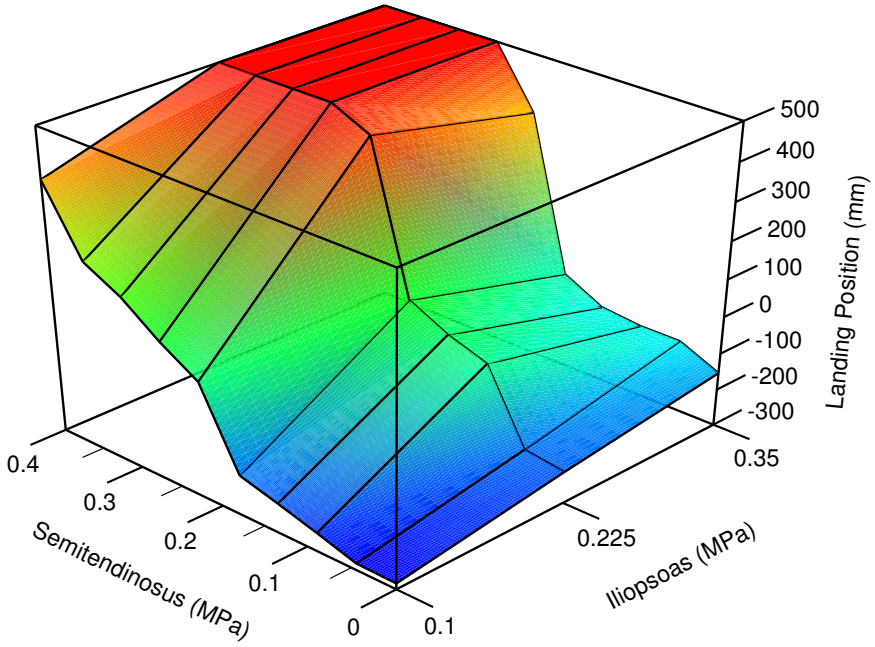

Figure 2.5: Relationship between muscles iliopsoas and semitendinosus during hopping in different angles.

After comparative data between IL and ST, the influence of gastrocnemius on directional change was measured. Setting IL and ST pressures at 0.25 MPa and 0.15 MPa, respectively, we calculated the average and standard deviation of 25 jumps for 6 different pressures at GA, as shown in Fig. 2.6. Following this experiment, we measured the contribution of GA pressure to angle variation at ankle and ground contact, as seen in Fig. 2.7.

The left dashed line at the graph indicate the point where the transition from digitigrade to plantigrade stance happens, while the right dashed line indicates angles where the hindlimb collapses. The criteria for defining these two thresholds is when the ankle touches the floor and when the angle at the ankle reaches 160 degrees, respectively.

Using data from previous figures, we estimated a relationship between ST pressure and landing position. Owing to better results compared to the polynomial approach, we decided to use a Boltzmann

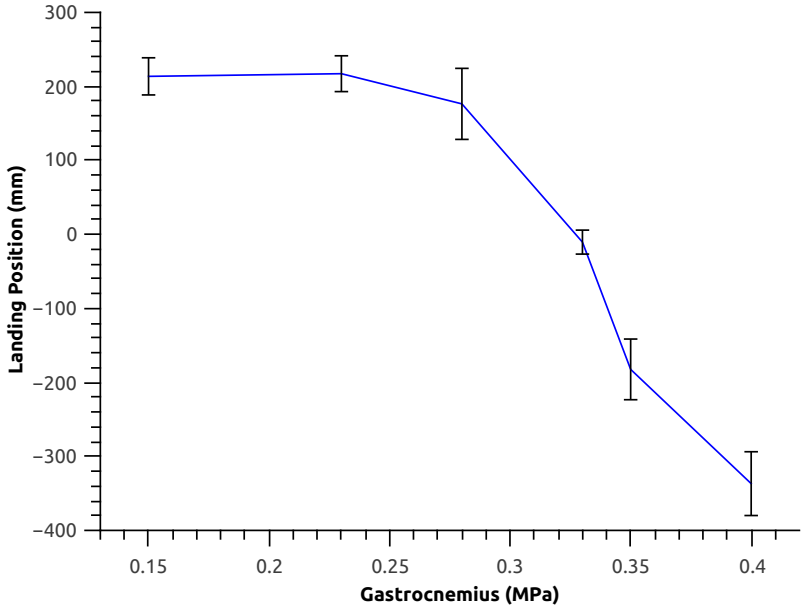

Figure 2.6: Landing position during hopping with different GA settings.

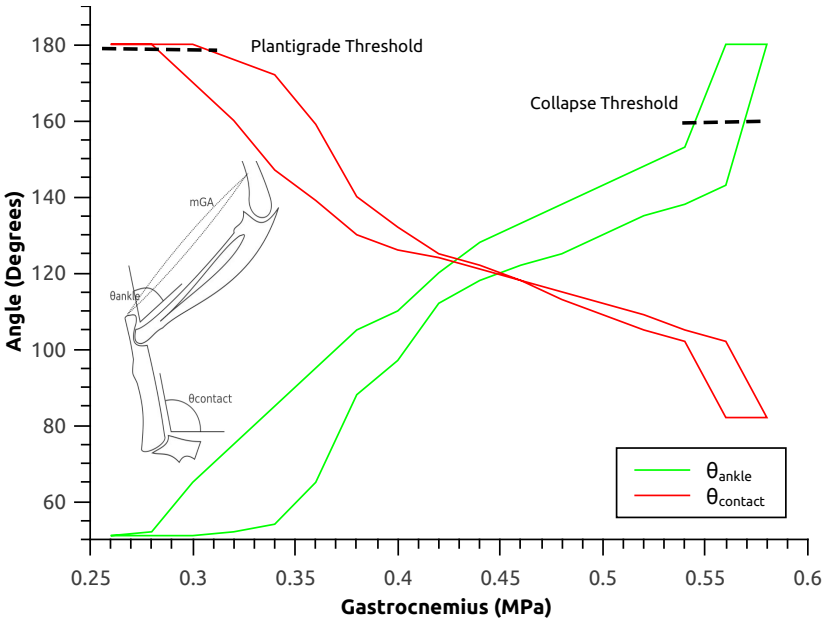

Figure 2.7: Angles and hysteresis for ankle and ground contact for GA changes.

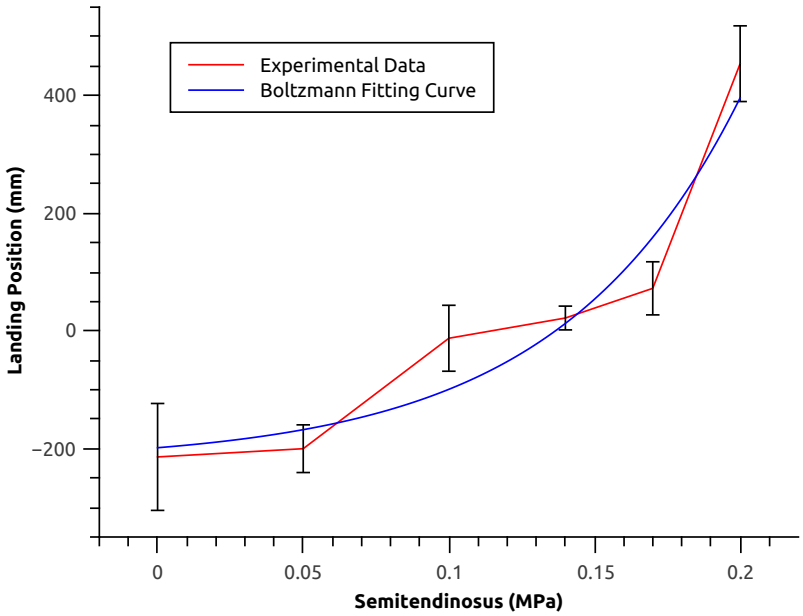

Figure 2.8: Boltzmann fitting defining relationship between semitendinosus and landing position.

based correlation equation of the available data set:

$$X_{(p_{ST})} = A_2 + \frac{A_1 - A_2}{1 + e^{(p_{ST} - p_{ST}0)/dp_{ST}}} \tag{2.6}$$

where $X_{p_{ST}}$ is the landing position, A_1 the lower limit, A_2 the upper limit, $p_{ST}0$ is approximately half of the pressure amplitude and dp_{ST} is the pressure range. The plotted curve can be found in Fig. 2.8. For the actual experiment, a lookup table relating pressures and landing positions was used, simplifying the control method and avoiding logarithmics at programming level.

Finally, using this same curve we performed a sequential jumping experiment, changing landing position parameters. Results for this final experiment can be found in Fig. 2.9, where we perform 72 jumps, defined arbitrarily. The two horizontal dashed lines indicate the points where the foot lands on the slope.

2.4 Discussion

The main objective of this work is to give a roboticist approach on a feline hindlimb muscular role during hopping. Analyzing pressure data from Fig. 2.4 and comparing with the activation pattern (Fig. 4.5), we can notice that the contraction of AB (hip extensor) seems to increase the tension of its antagonist, IL (hip flexor). The importance of IL before the beginning of the jump in our robotic hindlimb is to keep the hip joint in a centered position, where less pressure would result in a standing stance with the body slightly tilted backwards.

2.4.1 Iliopsoas and Semitendinosus Roles

Combining this pressure data with the relationship between IL and ST (Fig. 2.5), we can conclude that increasing the pressure of either muscle results in a positive foot placement. While a higher contraction on iliopsoas naturally brings the foot forward, since this muscle is the hip flexor, we observed that the increase in semitendinosus pressure rotates the hip backwards, thus bringing the center of gravity to the back and inducing sagittal rotation of the full system in mid-air.

While hopping with ST pressures greater than 0.1 MPa the behavior of the IL muscle was not continuous. At these pressures, higher pressures at IL did not necessarily result in crescent foot placement. We speculate that at high IL pressures (0.35 MPa) the increase in ST pressures creates a knee flexing torque, preventing an advancement on the foot placement. With low IL pressures the same does not occur, due to the lower hip flexion torque.

2.4.2 Gastrocnemius Role

On the GA muscle, the opposite phenomenon was observed. Increasing GA pressure resulted in a negative foot placement, and we suggest that the extension of the ankle combined with the flexion of the knee brings the center of gravity of the leg to the back, as seen in Fig. 2.6, thus rotating the system backwards.

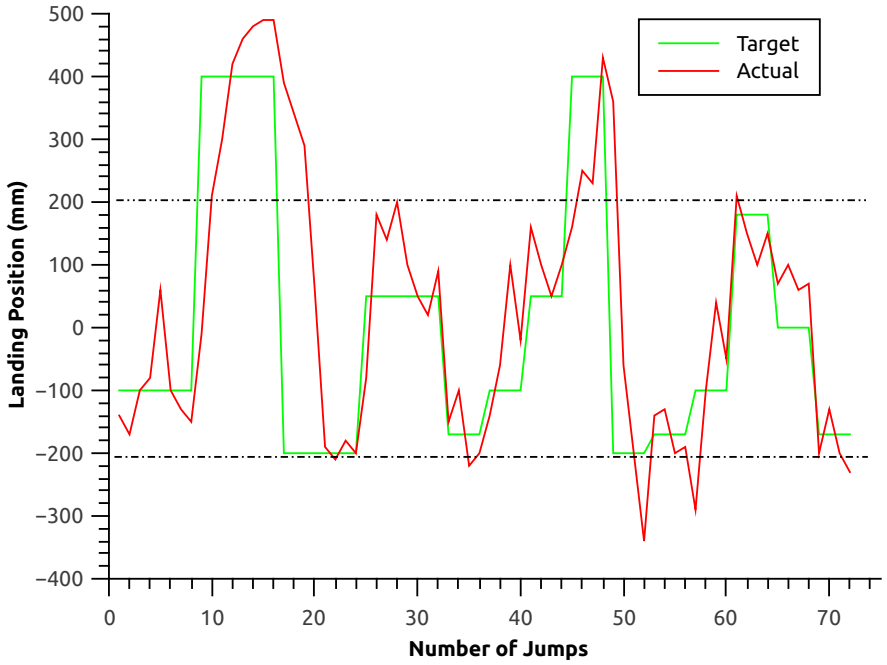

Figure 2.9: Jumping experiment with 72 sequential jumps and their target value.

Although it would be possible to control the hopping direction through gastrocnemius pressure, altering gastrocnemius pressure has a critical shortcoming for the hindlimb stability: As seen in Fig. 2.7, different pressures for gastrocnemius result in different attack angles. At one extreme, we have a plantigrade landing, which is not very efficient dissipating potential energy from the jump, while at another we have an ankle joint locked at 180 degrees, which simplifies the leg as a 2-link system, being also degrading for energy dissipation.

2.4.3 Control over Landing Position and Locomotion

Although biological data on how cats change muscular activation for different jumping directions is scarce, we propose that different tension on the ST muscle largely contributes to a better control over feline leaps.

Using the Boltzmann correlation based control of semitendinosus' pressure from Fig. 2.8 we performed a hopping experiment. The hindlimb sequentially hopped 72 times, tracking a target value for

landing position, as seen in Fig. 2.9. The error present in this method is a strong indicative that, combined with the ST tonal difference, other muscles could also be co-activated, hence the highly complex biological structure.

This approach widens our view for the possibility of correlating jumping direction control with specific gait patterns, such as pronking and bounding. The possibility of using directional control on fore and hindlimbs on a quadrupedal robot to reproduce these gait patterns would possibly make robot locomotion easier.

2.5 Conclusions and Future Works

The morphological complexity of animals is a conundrum which roboticists are still scratching the surface, and this work delves into the problem aiming to provide more clarity on the subject.

We built a biomimetic hindlimb with an experimental platform for hopping. After creating a muscular pattern for vertical jumping, we systematically tried different pressure configurations for monoarticular and biarticular air muscles, finding a relationship between muscular activation and landing position in a series of jumps. Although gastrocnemius, iliopsoas and semitendinosus contribute to the sagittal rotation, the most reliable way for changing hopping direction was shown to be through semitendinosus tonus control.

We performed experiments applying the proposed tonus control, and the proposed method may offer a possible explanation for a directional change of a real feline jump, and the result could be extended to gait pattern explanation, such as bouncing and pronking gait, where the average speed could be controlled by semitendinosus activation.

Future works will focus on reproducing phenomena observed on feline-related publications[11 8], associating muscular activation to air pressure, hoping to provide a constructivist feedback to biologists.

Integration of the hindlimb with the full body Pneupard will provide us with a full biomimetic platform, being the closest robotic platform to date to mimic the *Felidae* biological system (considering morphology, muscular redundancy or number of active muscles). This platform will be used to

validate the aforementioned controlling method, aiming to control Pneupard direction during locomotion.

This chapter is based on the article:

Rosendo A, Liu X, Shimizu M, Hosoda K. "Stretch reflex improves rolling stability during hopping of a decerebrate system", Bioinspir. Biomim., submitted[9].

3

Stretch reflexes stabilization on frontal plane hopping

During human hopping, attitude recovery can be observed in both sagittal and frontal planes. While it is agreed that the brain plays an important role on leg placement and muscular activation, low-level feedback (stretch reflex) effect on frontal plane stabilisation remains unclear. Aiming to better understand stretch reflex contribution to rolling stability, experiments were performed on a biomimetic humanoid hopping robot. Different reflex responses were used upon touching the floor, ranging from no muscle response to long muscle activations,

and the effect of a delay upon touching the floor was also observed. As a conclusion, the presence of stretch reflex brought the system closer to a stable, straight hopping. The presence of an activation delay did not affect the results, where both cases (with or without delay) outperformed the case without reflex response. Therefore, these results emphasise the importance of low-level control on locomotion, where the body prescinds from brain created signals to stabilise.

3.1 Introduction

Understanding how animals move has been the main objective of several researches in the past 100 years[40]. A better understanding of how our body works not only allows us to solve problems which may occur in our biological systems, but also apply such insights on new technology development. Through nature observation (bioinspiration), inventions such as air planes[52] were conceived, and roboticists have been trying to mimic animal behaviour for many years[27,6], in an attempt to grasp the source of locomotion's stability.

Hitherto, it is understood that animals control their bodies through a combination of higher-level and lower-level control signals[42]. The former is originated from the brain and has a longer travelling distance to the actuator (muscle), having longer delays (above 300 ms for visual stimulus-manual response trials[18]), being the latter a stretch reflex response, generated by muscle spindles upon sensing length changes on the muscle fibre. This response, faster than brain signals (below 50 ms)[65], has come to attention of researchers for its positive effects on body stability. In[43,26], a decerebrated cat walking on a treadmill uses stretch reflex to stabilise its walking pattern, while in[32] feedback role on high-frequency walking of insects is explained.

Experiments have proven benefits from proprioceptive feedback on human standing stability[17,10], and, during human walking, stretch reflex contributes to ankle extensor activation during early stance phase[58]. Moreover, biological experiments with hopping humans infer that humans choose hopping frequency to maximise effect of stretch reflex[38] and that H reflex suppression during landing changes

muscular behaviour from spring to damper[13].

While in biological experiments it is difficult to isolate brain signals from lower-level responses in hopping humans, simulations tackle the problem by recreating a simplified version of such experiments. In[21], a simulation of a hopping two-segment leg takes place with muscular activation generated by proprioceptive sensory feedback. In[61,25], using an opposite approach, simulations adopt a feed forward control, stabilising through irregular terrain while exploiting muscular properties. Haeufle *et al.*[24] suggests a simulation combining feed-forward control with proprioceptive feedback responses, adding disturbances to the simulation and analysing individual contributions from each control alternative.

Real world dynamics involve lots of noise, asymmetries and unknown disturbances, which can not be fully mimicked in simulation environments. Muscular properties are usually approximated by a Hill muscle model, which does not account for coupling between activation and force-velocity properties[44] and body-environment interactions are usually poor. The field of biomimetics aims to imitate life with artificial systems, allowing experimental settings which thus would not be biologically possible. In[9], an artificial tentacle robot imitates the movements of an octopus, while on[55,54] a decerebrate biomimetic cat walks on a treadmill with different muscular activations.

In this work, we perform hopping experiments with a robot using artificial pneumatic muscles. Such muscles perform similarly to biological muscles in many aspects (force-length relationship, radial expansion on contraction[4]) and allow us to analyse stretch reflex contribution during hopping. Different from other bipedal hopping experiments (biological or biomimetic), we evaluate the contribution of soleus muscle (ankle extensor) on the rolling stability of humans. Although stretch reflex has been studied in hopping before[64,35], its contribution to rolling stability has never been approached.

Our biomimetic robot hops in place, landing from different angles between -5° and 5°, and the angle at lift off is equally recorded and compared. We found that the use of stretch reflex improved the lift off angle output. Moreover, hopping with a delay between touching the floor and the stretch reflex response still has better results than the lack of reflex upon touching the floor.

In Section 3.2 we introduce the robot design and the program emulating hopping sequence and stretch reflex. We also describe the experimental setting used to perform experiments. While on Section 3.3 we show experimental results, on Section 3.4 we discuss those results and conclude this work.

3.2 Materials and Methods

Aiming to achieve biologically representative results, the human morphology was replicated considering the musculoskeletal structure with the most representative muscles on human legs. Understanding how such muscles interact with the environment requires that our chosen actuators mimic their behaviour, thus eliminating electric motors from our design options. Pneumatics and hydraulics are known for offering some compliance, with special attention to air muscles, which have been used for many years as a successful replacement of biological muscles in robots [27,6,55] and rehabilitation [68].

3.2.1 Hopping algorithm

To generate a hopping sequence the robot must be capable of interacting with the environment. Sensing the moment that it lands, the robot should wait for the lowest point to be reached to supply air to the extension muscles, and later be capable of restoring the muscles to the original landing activation pattern, preparing for the next landing. This way, the hopping is produced by a finite-state machine algorithm where 3 states are present:

- Landing state: In the landing state, the robot adjusts the muscular pressure on every muscle to reach a predetermined value, which is the same on every landing condition. This state is the initial state of every experiment.

- Complying state: When the robot detects the touch of the foot against the floor (change of signals on touch sensor) the complying state is activated (Fig. 3.1 (a)). In this state, the robot supplies air to the soleus muscle for a predetermined time (T_s) and closes the muscle, sampling

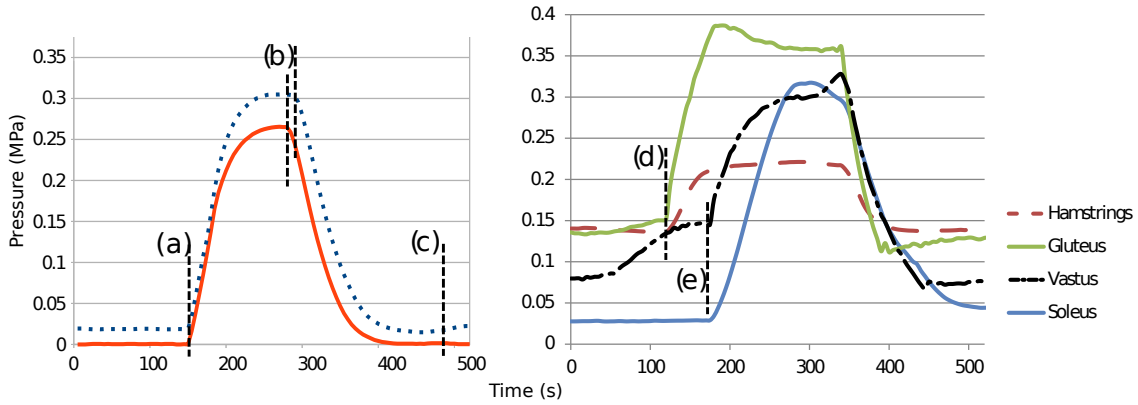

Figure 3.1: Graph with muscles during hopping. On the left we can see the behaviour of right (dotted blue) and left (solid red) sensing soleus. Upon touching the floor (a) they are both supplied with air for a few milliseconds and then closed. When their pressure reaches its peak (b), which may be different for different legs, the supplying state is activated, later activating again the landing state (c). The supplying state acts on proximal muscles first (d), activating distals later (e).

its inner pressure while the leg deforms with its weight. The end of this state is reached when the pressure inside soleus muscle reaches its peak (Fig. 3.1 (b)), which is described as:

$$\frac{\partial P_s}{\partial t} = 0$$

where P_s is the muscle pressure inside soleus muscle. The peak in the pressure curve means that the maximum deformation was achieved, activating the next state.

- Supplying state: During this state the major extensor muscles are activated for a predetermined time (Fig. 3.1 (d) and (e)), generating an upward movement. The timing sequence of each muscle during explosion is detailed in previous publications[27], and after the robot loses contact with the floor the landing state is activated (Fig. 3.1 (e)), which will once again adjust the muscles for landing.

During hopping, all the muscles have a constant pressure, acting as passive springs. Data from roll angle, pitch angle, hopping state and internal pressure on muscles are sampled to a computer.

The predetermined time of muscular activation (*e.g.*, $T_s = 30$ would supply the soleus for 30 ms, closing the valve after that) can be adjusted on every muscle, and a second timer, called delay timer, can

be added to simulate a delay between the trigger and the muscle response. The finite state programming allows right and left legs to respond independently, simultaneously or with inhibition between them.

Hopping experiments were performed by releasing the robot on the floor from many different attack angles, forcing the robot to develop the 3 different states mentioned above. One single experimenter was adopted for every trial, using the same pitch attack angle for every jump and releasing the robot from approximately the same height of 25 cm between foot and floor, which was defined for being comfortable for the experimenter to perform more than 100 jumps while having a good jump height. The experimenter was instructed to drop the robot from random initial roll angles (without any angular velocity or acceleration), where both touching down angle ϑ_t and lift off angle ϑ_l are compared after the jump. After the contact between the robot and the floor was lost, the experimenter was instructed to grab the robot midair and prepare to release the robot from another random roll angle.

The results are compared by plotting the initial touch down angle ϑ_t in the horizontal axis and the lift off angle ϑ_l in the vertical axis. Since we are interested in measuring the recovering capability of the system, jumps will be graded by the following procedure:

$$\Delta = \begin{cases} \vartheta_t - \vartheta_l, & \text{if } \vartheta_t \geq 0 \\ \vartheta_l - \vartheta_t, & \text{otherwise} \end{cases}$$

where positive values indicate recoveries and negative values indicate worsen conditions. Special attention should be paid to values close to the straight position ($0°$), since in this region this evaluation considers changing hopping direction as a recovery measure.

During hopping, the position of the centre of gravity (COG) is very important to determine the possibility of rolling stabilisation, where a COG located outside the area below both feet should make stabilisation impossible without abduction. Considering the COG height of 780 mm and distance between feet of 200 mm, $\vartheta_{max} = \arcsin(100/780) = 7.36°$ is the angle at which the COG would fall entirely on one foot. The hopping range between $-5°$ and $5°$ was chosen, assuring that stretch

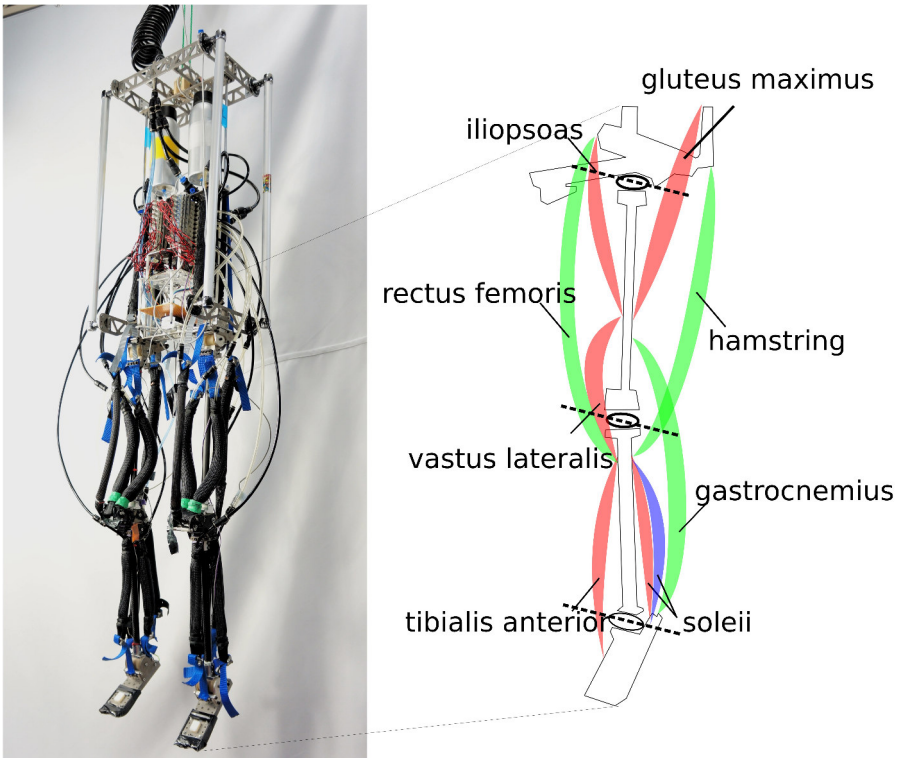

Figure 3.2: Picture of robot with pictogram detailing muscles on each leg. The robot has pneumatic valves, micro controller and battery on board, and the leg structure has biarticular muscles in green and monoarticular muscles in red, controlling 3 degrees-of-freedom. The additional soleus muscle, in parallel (blue), has the sole purpose of detecting pressure differences during landing.

reflex contribution could be evaluated while allowing individual analysis within 5 groups: $(-5°,-3°)$, $(-3°,-1°)$, $(-1°,1°)$, $(1°,3°)$ and $(3°,5°)$.

3.2.2 Robot design

The robot has 9 air muscles on each leg, from which 3 are biarticulars and 6 are monoarticulars, controlling 3 degrees of freedom in each leg (ankle, knee and hip joints). With an overall weight of 7.8 kg, height of 1.3 m and a 200 mm width, it is depicted in Fig. 3.2.

One of the soleus muscles does not contribute as an extensor, being solely used as a sensor, detecting pressure changes during landing. With the intent of producing a lightweight testing platform, the robot uses light materials on its body, such as magnesium alloy, carbon fibre and ABS plastic. The

pneumatic valves, micro controller and battery are located inside the torso of the robot, connected by a tether which communicates and supplies compressed air. Two small air tanks act as pneumatic capacitors, offering pressure stability between jumps.

The micro controller communicates at 200Hz, powered by a 32-bits 72MHz ARM MCU (STM32F103, ST Microelectronics), while sampling data from 2 touch sensors at the tip of each limb, 2 pressure sensors on each soleus muscle, a three axis accelerometer and two gyroscopes. All these sensors act, respectively, to identify the moment the robot touches the floor, the stretch response on the soleus muscle and to provide roll/pitch angle information through a complementary filter between accelerometers and gyroscopes. More information on the humanoid robot specifics and sensing are located in the appendix A.

3.3 Results

Aiming to better understand the contribution from stretch reflex, experiments were performed with 5 different cases: No reflex ($T_s = 0$ ms), Reflex-30 ($T_s = 30$ ms), Reflex-70 ($T_s = 70$ ms), Reflex-100($T_s = 100$ ms) and Reflex-130 ($T_s = 130$ ms), simulating different reflex strengths upon touching the floor. In this publication, we focus on cases using contralateral muscular inhibition, where afferent signals from the ipsilateral extensor muscles suppress stretch reflex on the opposite leg.

In Fig. 3.3 the results of 5 different hopping experiments are shown. Each of these experiments had more than 100 jumps (top right corner of graphs), and averages were calculated for each case in the proposed 5 different groups (red crosses). Starting from the No Reflex condition, we could notice a certain linearity among the averages (red crosses), where jumps to both sides maintain the same orientation (a). Upon adopting Reflex-30 it is noticed that the inclination of the results decreases (b), approaching the horizontal axis. As a consequence, results for $\Delta\vartheta$ increase (f-g), with more hops passing the $\Delta\vartheta = 0$ threshold. Aiming to understand this mechanism, different reflex cases (70 ms, 100 ms and 130 ms) were tested and their results plotted (c-e). It was found that the trend kept true, with values approximating even more the horizontal axis. Although hopping height was not evaluated, the experimenter

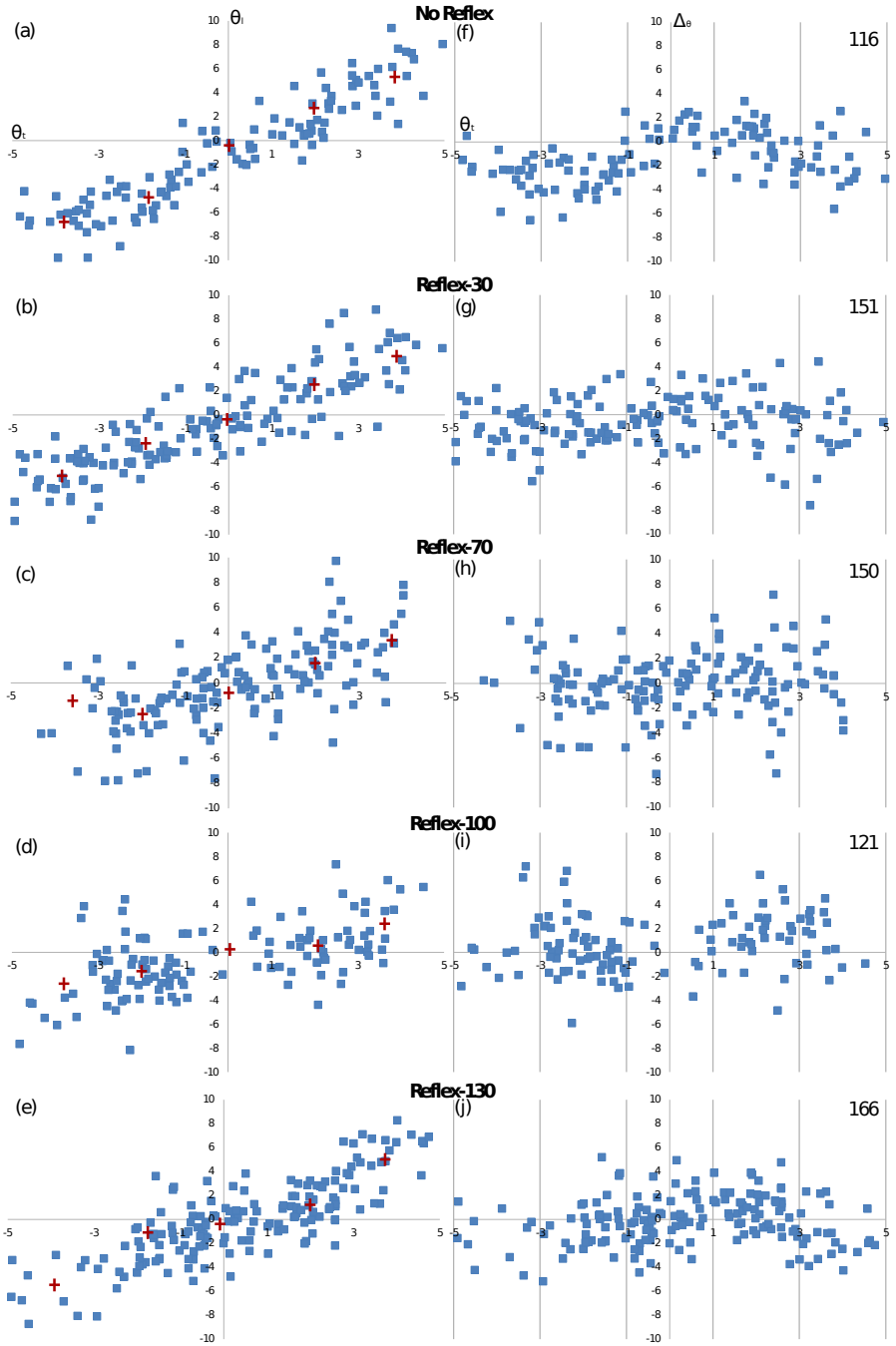

Figure 3.3: Hopping experiments result, where on the left side (a-e) we have ϑ_t versus ϑ_l and on the right side (f-j) we have a performance evaluation with ϑ_t versus $\Delta\vartheta$. As the stretch reflex gets stronger, the inclination of the lines passing through the average points (red crosses) decrease (a-d), increasing again at the Reflex-130 case (e). As a consequence, the number of points above the $\Delta\vartheta = 0$ line increases, where initially on the No Reflex (f) case the majority of points is negative and in the best case, Reflex-100 (i), most of its points are above the axis.

observed that increasing the reflex response degraded this height, where the Reflex-130 case had the worst hopping height.

Literature on human stretch and Hoffmann reflex[65] shows that a delay between the muscular excitation and the reflex response exists. Based on the previous experiments, four new conditions were created, considering a 15 ms delay between touching the floor and starting the stretch reflex response: Delay-30, Delay-70, Delay-100 and Delay-130.

In Fig. 3.4, these four new conditions are compared with the previous No Reflex condition. Similarly to previous experiments, the No Reflex case had the highest inclination, with every other case being closer to the horizontal axis. Once again, the performance of Delay-130 was the worst among delayed cases when it comes to hopping height, and the experimenter added that it was worse than Reflex-130.

The average and standard deviations of 5 groups from these 9 cases were taken and compared using a two-tailed unpaired t-test with a 95% confidence interval. Variance ratios were compared to F values and variances do not differ significantly. This approach was chosen over an inclination analysis of a linear regression (such as least squares estimation) for allowing individual analysis of groups, where asymmetry can be properly represented.

3.4 Discussion

An analysis of stretch reflexes during bipedal hopping has been done clinically[65,38] and mathematically[25,24], but none of these researchers considered the stability contribution to the frontal plane. The fact that separating brain signals from muscular feedback responses during hopping is clinically difficult explains why such topic is rarely approached in physical experiments. In simulation environments, on the other hand, approaching this topic could be possible by simulating muscular responses with different landing angles on a frontal plane. Although possible, the lack of real world disturbances in this approach would make a physical experiment the best candidate to realistically reproduce observed phenomena.

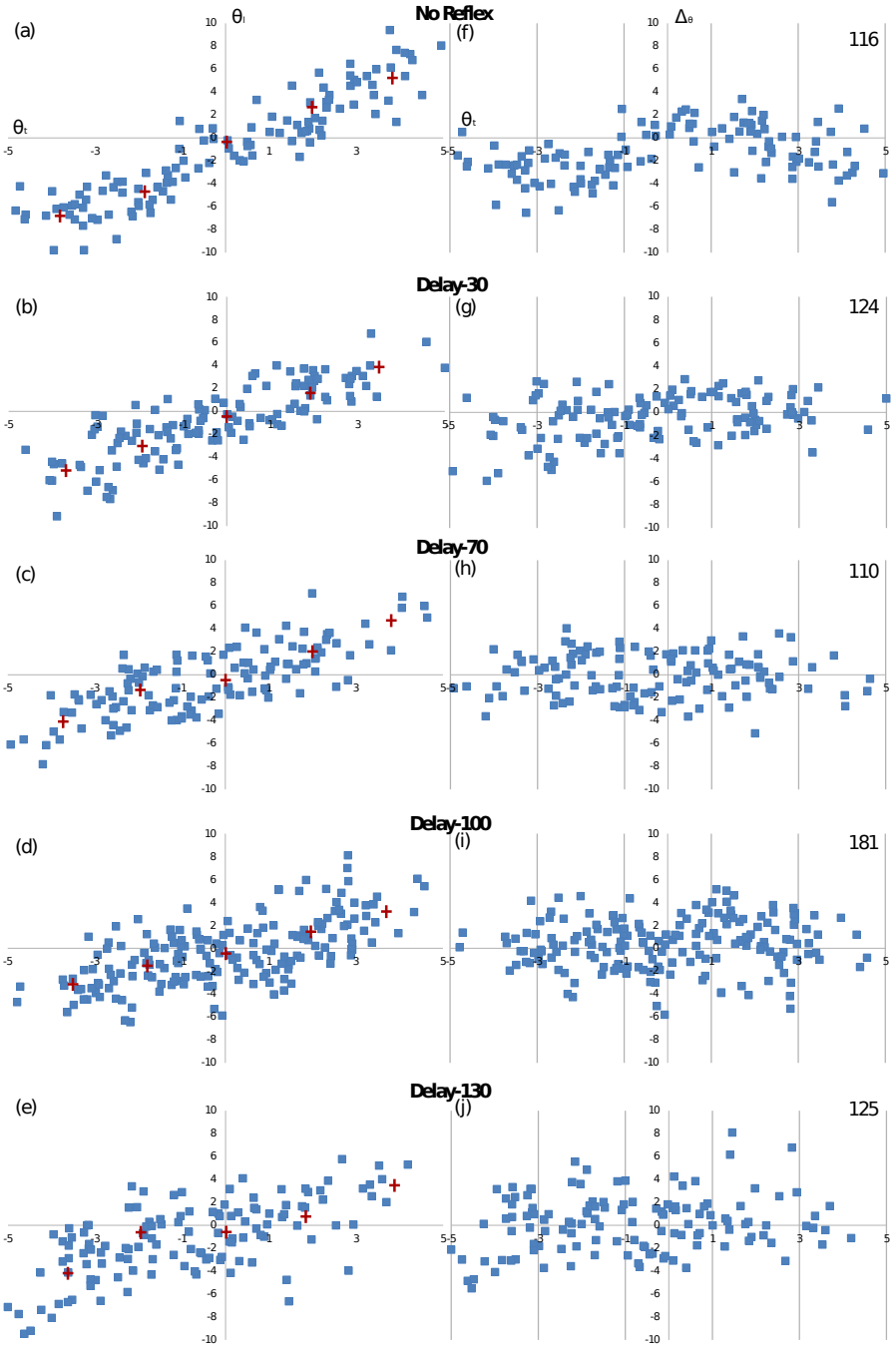

Figure 3.4: Hopping experiments considering a 15 ms delay before reflex onset, where on the left side (a-e) we have ϑ_t versus ϑ_l, and on the right side (f-j) we have a performance evaluation with ϑ_t versus $\Delta\vartheta$. As the stretch reflex gets stronger, the inclination of the lines passing through the average points (red crosses) decrease (a-e). As a consequence, the number of points above the $\Delta\vartheta = 0$ line increase, where initially on the No Reflex (f) case the majority of points is negative and in the cases Delay-100 (i) and Delay-130 (j) we can see the best results.

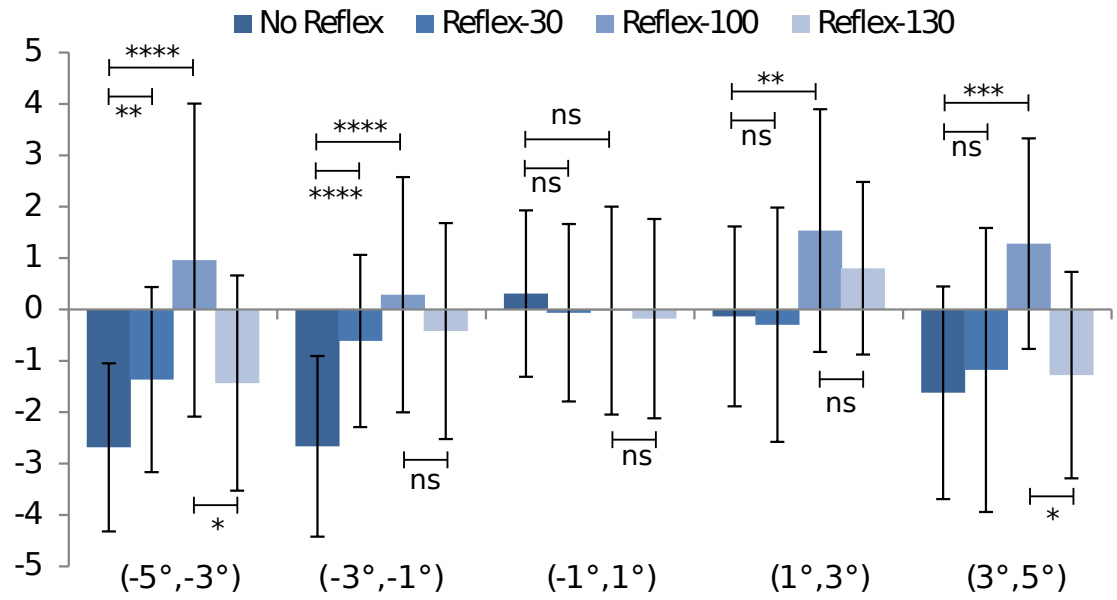

Figure 3.5: Comparison of $\Delta\vartheta$ performances between No Reflex, Reflex-30, Reflex-100 and Reflex-130 for the 5 proposed angle groups. Higher averages indicate better hopping performance. Error bars denote standard deviations. The statistical significance was measured between 5 groups and the symbols represent p < 0.05 (*), p < 0.01 (**), p < 0.001 (***), p < 0.0001(****) and n.s. for non-significant in t-tests.

3.4.1 Stretch reflex improves rolling stability

During the first experimental phase (Fig. 3.3) it was possible to notice that as the reflex response increased, the inclination of the line formed by the averages decreased. A comparison between the averages of the performance of each jump ($\Delta\vartheta$) with their respectives standard deviations is shown in Fig. 3.5. As it can be seen, an increase in the stretch reflex strength creates a similar effect on the hopping performance $\Delta\vartheta$. The trend that exists from No Reflex to Reflex-30 (only jumps to one side are statistically significant, with $p < 0.01$ and $p < 0.0001$) is reinforced by the comparison between No Reflex and Reflex-100, which is only non-significant between $-1°$ and $1°$. Moreover, Reflex-100 is proven to be the best case, where the case Reflex-130 degrades stretch reflex response in both extremities ($(-5°,-3°)$ and $(3°,5°)$, $p < 0.05$).

Although the claim that the presence of the COG closer to one leg would allow a bigger reaction force in the opposite direction is true, such effect is also present during the No Reflex case. While

bipeds have this advantage over monopods, this does not explain the superiority from Reflex versus No Reflex cases. We hypothesise that the physical explanation for this phenomenon is that the body, without any brain-generated signal nor pitch/roll information, corrects rolling by activating leg muscles through reflex response upon touching the floor. The implications of this assertion would be that decerebrate animals, if capable of hopping in place, would have a frontal plane stabilisation facilitated by such mechanisms.

In Reflex-30 case, only one side (negative) had statistically significant results. Robotic asymmetry may play a role on this, since both legs are not equal, and its effects on the experiment will be discussed in *Study limitations*. The Reflex-130 case was inferior to the Reflex-100 in both extremities, being non-significant in the middle zone. A possible explanation for this is that an extremely long reflex activation period interferes with the complying phase, resulting in a smaller amount of stored gravitational energy. In analogy with spring stiffness, Reflex-130 behaved as an overstiff spring which could not bounce properly, not correcting the posture.

In[13], the reflex suppression is compared to a damping unit. Although apparently diverging from our findings, where small reflexes created higher jumps, those results are actually convergent, since during landing (without a posterior jump) the stored energy is lost. Thus, the proposed damping unit must be associated with a soft spring, being suppressed in case of a countermovement jump (involving stretching muscles, similar to our No Reflex case and well described in[1]). During hopping, both results converge to a higher muscle stiffness produced by reflexes.

While hopping within $(-1°, 1°)$ range is very interesting when control stability is desired, when studying roll angle correction through stretch reflex this region did not yield good results. Small angles allow the robot to hop in any direction, and the need for rolling correction does not exist, being the stretch reflex an overcompensating measure. A higher average found in No Reflex cases may indicate that in straight hopping mutual inhibition emerges as a plausible solution, suppressing reflexes in both legs. Since statistical non-significance was observed between these results, this hypothesis would have to be verified in future works, with new experiments exploring this possibility.

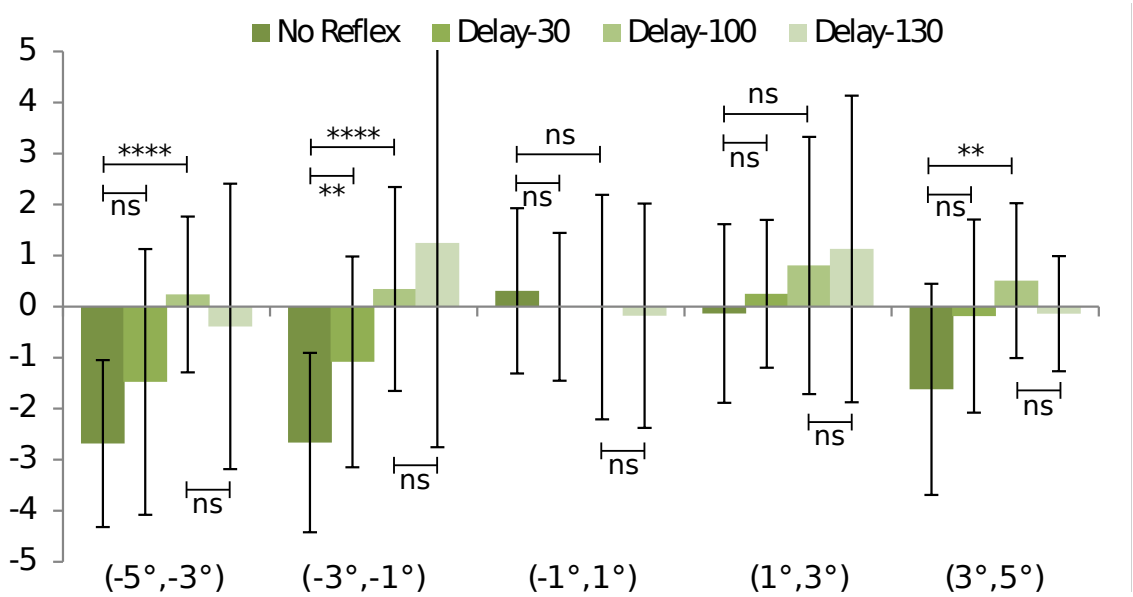

Figure 3.6: Comparison of $\Delta\vartheta$ performances between No Reflex, Delay-30, Delay-100 and Delay-130 for the 5 proposed angle groups. Higher averages indicate better hopping performance. Error bars denote standard deviations. The statistical significance was measured between 5 groups and the symbols represent p < 0.01 (**), p < 0.0001(****) and n.s. for non-significant in t-tests.

3.4.2 Delay presence outperforms lack of reflex

In Fig. 3.6 we can see a comparison based on results shown in Fig. 3.4. Similarly to the previous comparison, cases No Reflex, Delay-30, Delay-100 and Delay-130 are compared for the same 5 angle groups.

Initially, a comparison between No Reflex and Delay-30 yields only one statistically significant t-test ($(-3°,-1°)$, $p < 0.01$) with the delayed case outperforming the former. Since average values from Delay-30 indicated superiority when compared to No Reflex, a stronger case (Delay-100) was compared to the No Reflex case.

Here, a strong $p < 0.0001$ significance was found for one side entirely $(-5°,-1°)$, while for the other only the region $(3°,5°)$ had $p < 0.01$. Hence, the stretch reflex corrective behaviour still holds true when a delay is applied, similarly to human beings. Although human stretch reflex is greater than 15 ms (in [65] values between 30 and 40 ms can be seen), this value was used considering the intrinsic delay of air muscles. Upon opening pneumatic valves, compressed air takes longer than a biological

soleus muscle to reach its peak force.

As observed by the experimenter, the case Delay-130 had the worst hopping performance. Recalling an analogy to the spring made in the previous section, the case Delay-130 acts as a very soft spring for 15 ms, complying with the gravitational force, and suddenly stiffening for 130 ms. Although clearly superior to the No Reflex case in roll angle correction aspects, this unnatural hopping strategy produced a very small ground clearance while hopping. Comparisons between this case and Delay-100 were inconclusive, with all cases being statistically non-significant, which may also indicate that they are very similar in terms of $\Delta\vartheta$ performance.

3.4.3 Delayed versus undelayed cases

One final comparison between results shown in Figs. 3.3 and 3.4 is regarding which might be the superior case among delayed and undelayed cases. As observed previously, Reflex-130 had a better hopping height performance when compared to Delay-130 cases, and a possible explanation is the sudden change between soft and hard spring behaviours. As seen in Fig. 3.7, we compared Reflex-30 and Reflex-100 against Delay-30 and Delay-100 to understand if the presence of a delay may degrade roll stability.

Statistically, it was not possible to determine which case had superiority over the other (all comparisons had non-significance), which indicates that both delayed and undelayed cases are very close in terms of behaviour. This allows us to reach a conclusion that the presence of a 15 ms delay does not degrade, statistically, the outcome of hopping experiments, and thus any observed difference may be product of chance. Analysing average values, without any consideration for statistical significance, we may observe:

- All the cases in the range $(-1°,1°)$ performed similarly, which also holds true for No Reflex cases.
- Reflex-30 cases are superior to Delay-30 cases for hops to one side (negative region), while the opposite is true to the other side (positive region).

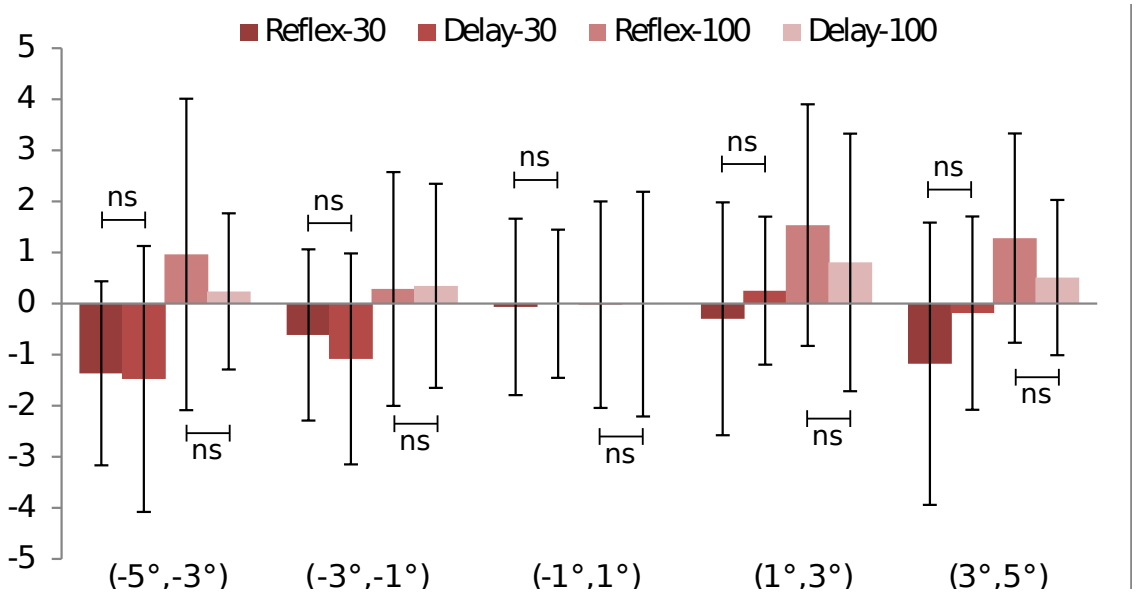

Figure 3.7: Comparison of $\Delta\vartheta$ performances between Reflex-30, Delay-30, Reflex-100 and Delay-100 for the 5 proposed angle groups. Higher averages indicate better hopping performance. Error bars denote standard deviations. Due to proximity of averages/high standard deviation all comparisons were considered non-significant (ns) in t-tests for a 95 % confidence interval. One-tailed comparisons would have rendered the same non-significance.

- Reflex-100 cases are superior to Delay-100 cases in almost all hops, being the only exception the $(1°,3°)$ range.

3.4.4 Conclusion

The contribution from a higher-level control (brain) on our stability is high. Even so, understanding how much our body contributes to our locomotion is essential to understand biological systems and, in the future, use this information to heal or to recreate ourselves (prosthetics, legged robots).

The presence of stretch reflexes helped frontal plane stabilisation in our biomimetic experiments, and the presence of a delay between touching the floor and reflex response did not degrade this phenomenon. In the future, experiments with decerebrate animals (deprived from vestibular and visual feedback) falling from a platform in different angles could help reproduce this work on a biological aspect. Whenever biological experiments are constrained by their own inner workings, biomimetic experiments emerge as the best interface between computer simulations and clinical trials.

This chapter is largely based on the article:

Rosendo A, Nakatsu S, Narioka K, Hosoda K. "Producing alternating gait on uncoupled feline hindlimbs: muscular unloading rule on a biomimetic robot", J. R. Soc. Interface, Vol. 28, pp. 351-365[35].

4

Stretch receptors contribution to alternating gait

Studies on decerebrate walking cats have shown that phase transition is strongly related to muscular sensory signals at limbs. To further investigate the role of such signals terminating the stance phase, we developed a biomimetic feline platform. Adopting link lengths and moment arms from an *Acinonyx jubatus*, we built a pair of hindlimbs connected to a hindquarter and attached it to a sliding strut, simulating solid forelimbs. Artificial pneumatic muscles simulate biological muscles through a control method based on EMG signals from

walking cats (*Felis catus*). Using the bio-inspired muscular unloading rule, where a decreasing ground reaction force triggers phase transition, stable walking on a treadmill was achieved. Finally, an alternating gait is possible using the unloading rule, withstanding disturbances and systematic muscular changes, not only contributing to our understanding on how cats may walk, but also helping develop better legged robots.

4.1 Introduction

Animal locomotion vastly outperforms any other human created locomotion method when it comes to adaptivity. Cats, dogs, horses and even humans can walk in many different conditions, keeping the same gait even at minor obstacles and random disturbances. The mechanisms for this higher stability are not fully understood, but scientists agree that a complex control method (brain) combined with a structure capable of adapting to unexpected disturbances (body) are two fundamental pieces in this conundrum.

Many researchers in the artificial intelligence field try to recreate intelligence with bio-inspired algorithms (*e.g.* neural networks, genetic algorithms, or refer[5] for more). However, irony abounds by the fact that the number of researchers trying to recreate legged locomotion with a true biomimetic morphology is extremely low. Apparently, conducting computer simulations has more controllable parameters than changing a morphology in contact with real environment, rich in noise and other disturbance sources. Hence, to close the gap between body and brain a better knowledge on the less explored biomorphology would be needed, and as a consequence, robotic locomotion could be improved.

Cats, from tiny domestic cats to big tigers, have baffled scientists over years. Although smaller than most of the dogs, any average domestic cat can climb trees, jump between wardrobes or run faster than their canine counterparts. Since this difference can not be attributed to higher computational power, considering smaller brain of cats, we are led to believe that the morphological difference between animals account for their higher specialization interacting with the environment.

Biologists have studied feline locomotion for many years: Engberg and Lundberg[15] studied EMG signals during unrestrained locomotion in cat hindlimbs, while Goslow Jr. et al.[23] identified joint angle and muscle length variations during the same. Herzog et al.[49,50] explores the roles of mono and bi articular muscles at the ankle joint and Wilson et al.[28,29] compares dissected forelimbs and hindlimbs from cheetahs and greyhounds, aiming to understand differences which could generate a nearly twofold maximum speed difference.

Beyond a muscular level, where only control outputs are observable, biologists hypothesize that the stepping cycle is regulated by afferent signals from peripheral sensory receptors, as stated by Pearson et al.[33]. The idea of sensors generating electromyographic (EMG) signals dates back to 1970, where Severin[57] proved that gamma activation of muscle spindles accounted for 50% of ankle extensors activity. The inputs for stable gait were well explained with decerebrate cats, where in[26] the absence of ground support reduced muscle activity in 70%, being fully restored when artificially loading the proprioceptors from extensor muscles. This have led scientists to believe that during stance phase more than half of the motoneuron inputs are due to afferent feedback, meaning that unloading the ankle is a necessary condition to start the swing.

With a vast amount of observed data on muscular pattern, joint angles and sensory feedback in cats, one may wonder why robotic performance is still so poor. Although there is a high degree of self-stability on musculoskeletal structures, only a few researchers try to mimic it. Among those trying to better understand animal locomotion replicating it, we could mention Yakovenko[69], which in 2004 developed a simulation with two walking hindlimbs supported by a linear constraint, with 6 muscles per limb. In 2005, Ekeberg[14] provides a groundbreaking simulation with 7 muscles per limb, 2 hindlimbs and a sliding strut as forelimbs, providing stable alternating locomotion while solely using the afferent based muscle unloading rule.

Real world implementations of such approaches are still rare: In 2006 and 2008, Quinn[3] and Tsujita[60] debut a pneumatic artificial muscle based quadruped robot with monoarticular muscles between joints, while in 2011 Hoffmann[34] and Kuniyoshi[70] were more through, also considering contributions

from biarticular muscles, famous for their role on energy transfer between joints[63]. Although these four robots explored muscular contributions, no considerations regarding sensorial unloading feedback were taken. On the opposite side of this sphere we can cite Maufroy's work[36], where the sensorial feedback was considered with no regards for the muscular structure, using servo-motors to produce joint torque.

Aiming to shed some light on biological locomotion the proposed rule is tested on a biomimetic robot, which adopts realistic link lengths, moment arms and significant muscles for locomotion. To replicate the biological muscle behavior air muscles were used, totalizing 7 active and 1 passive muscle per hindlimb. Similarly to Ekeberg[14], 2 hindlimbs are attached to a sliding strut and tested in a treadmill environment. While at Ekeberg the chosen animal was a domestic cat (*Felis catus*), in this work we choose as musculoskeletal model a cheetah (*Acinonyx jubatus*), in face of the little that is known regarding its locomotion.

The robot is capable of walking stably on the treadmill with a simple finite state programming using EMG data from cats to generate a muscular activation pattern. The only feedback source, a small force sensor on its foot, is responsible for stance-to-swing and swing-to-stance transitions. The unloading rule is adopted and successfully generates an alternating gait between hindlimbs, not requiring any kind of coupling between legs to maintain rhythmic behavior. Being the first real world biomimetic implementation of such biological rule, this same concept could help in the future on the development of more stable biped and quadruped robots. Differently from Ekeberg and Maufroy's works[14 36], different force thresholds and muscle contribution to stability are compared, going beyond just bringing Ekeberg's simulation to real life.

While in this first section we introduce the problem to be approached, section 4.2 explains the adopted methods, with design, construction and programming details. The third section describes the experiments adopted to validate our robotic stability, while in sections 4.4 and 4.5 the results are shown and discussed, respectively. Lastly, we conclude this work in section 4.6.

4.2 Methods

The main purpose of recreating a biological system is to perform experiments which can not be performed on the real animal. However, to assure that the performed experiment has any scientifical significance the amount of reproduced features must be great enough to replicate intended phenomena. This way, we focused on replicating the musculoskeletal system with force sensing capability, and no special attention was paid to other features (vision, fur, etc). Due to the low speed, the construction of the tail was also ignored.

4.2.1 Hindlimbs design

In [11], a comparison among members of the *Felidae* family is drawn, showing locomotion and morphologic similarities with felines ranging from 4 to 200 kg. Adopting link lengths from this work, combined with musculoskeletal information from [29], we opted for the creation of a 3-link hindlimb (femur, tibia and metatarsus) with 3 degrees of freedom and 8 flexion/extension muscles (as previously approached in [56]). These hindlimbs are attached to a hindquarter, which are fixed to a sliding strut to simulate a forelimbs-spine assembly. Although resembling a cheetah in structure, for aesthetic reasons we preferred to name it as a member of the *Panthera pardus* species, hence called Pneupard. A picture and CAD design image of the same can be found in Figs. 4.1 and 4.2.

From the 8 available muscles for flexion/extension, five are monoarticulars and three are biarticulars. The monoarticular muscles are biceps femoris (hip extension), iliopsoas (hip flexion), vastus lateralis (knee extension), soleus (ankle extension) and tibialis anterior (ankle flexion). All of them active muscles, with the exception of tibialis anterior. Although biceps femoris is not a monoarticular muscle *per se*, the small size of its moment arm around the knee directed us to a simplification, approximating it to zero.

The remaining three biarticular muscles are semitendinosus (hip extension and knee flexion), rectus femoris (hip flexion and knee extension) and gastrocnemius (knee flexion and ankle extension). Gas-

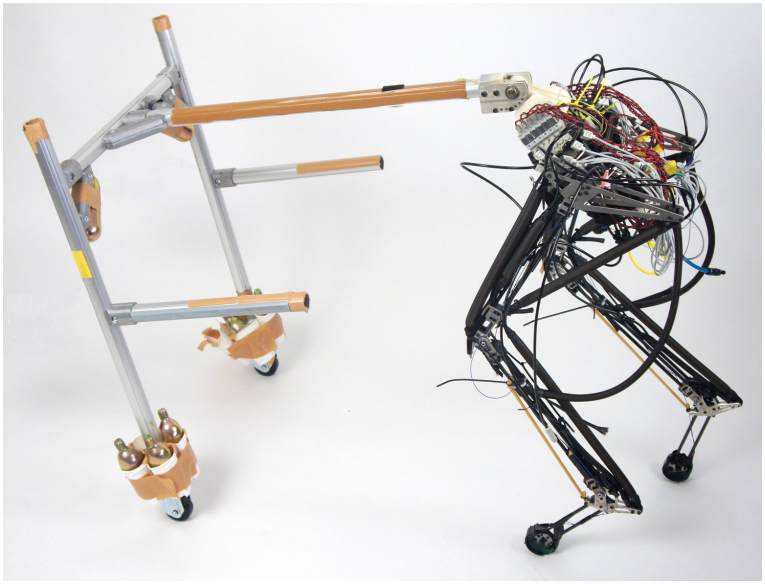

Figure 4.1: The robot possess hindlimb dimensions similar to a cheetah, with realistic moment arms to produce scientifically relevant locomotion during EMG-based muscular activation.

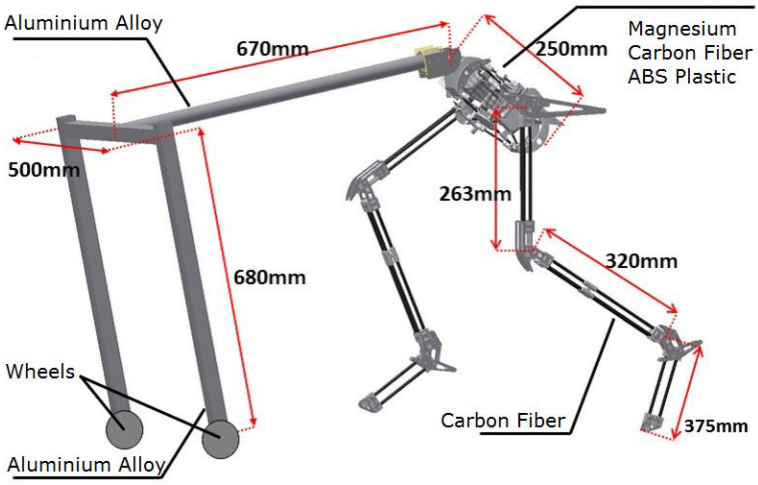

Figure 4.2: CAD design of Pneupard with important measurements depicted.

trocnemius and rectus femoris are known for transfering force between joints, according to[63]. Semitendinosus, on the other hand, has a flexor characteristic, as observed by Goslow[23], being solely used during phase transitions. Two additional muscles are fixed throughout the experiments, constraining adduction-abduction movements with a certain degree of compliance. If needed, movements of adduction (passive) or abduction (active) can be performed, imitating muscles such as gracilis, caudofemoralis or pectineus. A table with overall muscle lengths, adopted moment arms, nomenclature and articulation type can be found at Table 4.1.

Table 4.1: Pneupard's muscular specification

Muscle	Length[mm]	Max. Moment Arm[mm]	Articulation type
Soleus(SO)	170	61(ankle)	Monoarticular
Gastrocnemius(GA)	390	41(knee), 71(ankle)	Biarticular
Vastus Lateralis(VL)	145	27(knee)	Monoarticular
Semitendinosus(ST)	440	135(hip), 102(knee)	Biarticular
Biceps Femoris(BF)	320	150(hip)	Monoarticular
Rectus Femoris(RF)	330	47(hip), 22(knee)	Biarticular
Iliopsoas(IL)	230	47(hip)	Monoarticular
Tibialis Anterior(TA)	230	48(ankle)	Monoarticular

Aiming to provide a high fidelity between robot and animal, origin and insertion points were maintained, respecting muscular moment arms. A single exception was made during the attachment of the muscle iliopsoas, where in the animal it has origins on the animal's trunk, attaching on the proximal part of the femur. In our robot, we had to attach it in the distal part of the femur to share the same attachment platform as the other hip muscles. In Fig. 4.3 a schematic drawing represents the adopted muscles origin and insertion points.

4.2.2 Muscular consideration

The pneumatic artificial muscles are filled with air provided by 14 pilot operated on-off valves. A control method called hysteresis control[56] allows a certain degree of pressure control inside each muscle for different activation levels. The choice of on-off valves over proportional valves is due to the fact

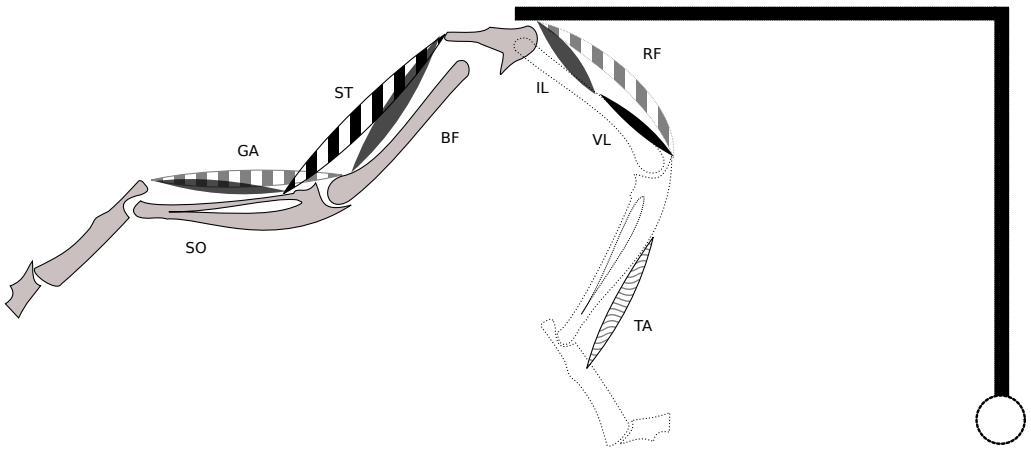

Figure 4.3: Diagram with Pneupard's musculoskeletal structure. Muscles in solid black are monoarticular muscles, while muscles in thick stripes are biarticulars. Right and left hindlimbs have different colors, passive muscles have a thin striped pattern and muscles related to adduction and abduction are not depicted on this diagram.

that, considering the same weight, it is possible to have higher flow rates with the former, allowing fast movements. Thus, the hindquarter-hindlimbs assembly weighs less than 3 kg (each hindlimb weighting less than 600 g) while having proportions of a cheetah. The maximum pressure used is 0.6 MPa, where our manufacturing process guarantees a life time of a few years, decreasing to months if used above 0.7 MPa. Due to our non-industrial manufacturing process, muscle length repeatability varies $\pm$ 5mm.

Adopting EMG signals from walking cats[15], similarly to Ekeberg's simulation[14], we constructed a finite state control with 4 distinct phases: Lift off, Swing, Touch down and Stance. Each phase has a predefined target pressure for each muscle, and the right and left hindlimbs are uncoupled. The initial phase is Touch down, where the microcontroller samples for activity on the force sensing resistor at the tip of the hindlimb. When stimulated, the state is switched to Stance, which lasts until the ground reaction force acting on the sensor decreases to a value below a predefined threshold, activating then the Lift off phase. The end of the Lift off phase happens when the contact between the sensor and the floor no longer exist, starting the Swing phase. Differently from Ekeberg, Pneupard's swing phase is solely based on a timer interrupt, not requiring a second sensor on the hip. After the specified time, the hindlimb enters Touch down phase again, waiting for floor contact.

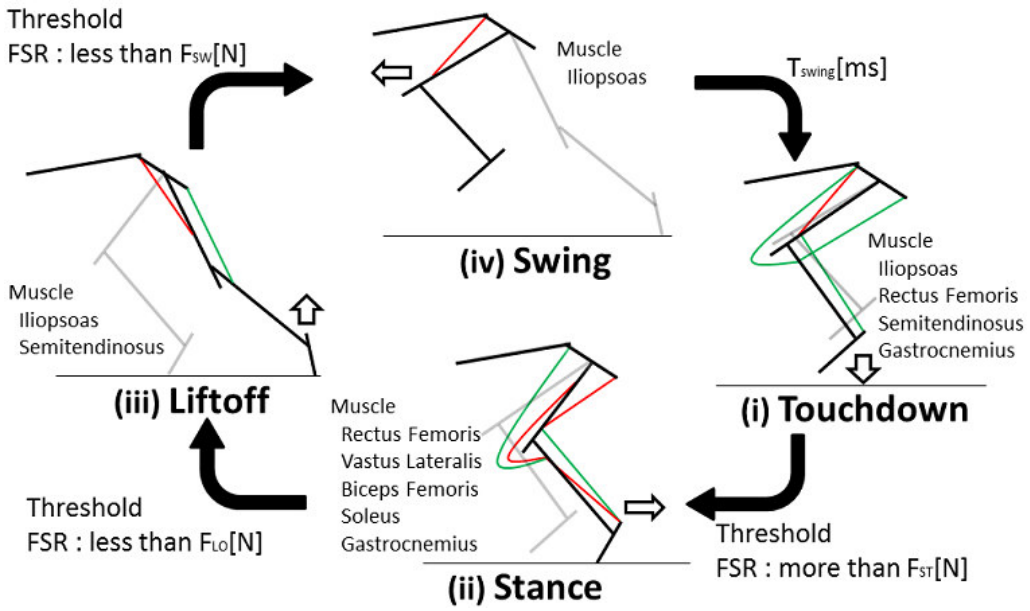

Figure 4.4: Four states of the finite state controlling on the hindlimbs. We can see the contribution of each muscle during each phase.

The design choice of not implementing hip angle as a swing limit parameter is based on biological data which proves that swing phase duration has low variance with different velocities (stepping frequency), as shown in [47]. The system could walk stably without this angle information, using a fixed 350 ms as transition timer. The four states of the adopted control method are depicted in Fig. 4.4. Since this work aims to prove that the unloading rule is capable of creating a stable locomotion in musculoskeletal systems, other sensors (gyroscope or accelerometer) were not adopted.

The adopted activation pattern for Pneupard is depicted in Fig. 4.5. Since biological muscles and artificial muscles have different properties, a fine tuning process (described in Experiments section) was required to translate the muscle signal into proper pressure signals. Contributions from higher-level controllers (brain) and lower-level controllers, such as spine-generated central pattern generators, were ignored in order to focus on the intended phenomenon of rhythmic gait through unloading rule in decoupled hindlimbs. The coupled hindlimb alternative was not tested, since it was proven in simulation that it did not improve the system behavior during unloading rule[14]. Moreover, coupled hindlimb controls are already broadly studied by the majority of roboticists (e.g.[3 60]), being the uncoupled con-

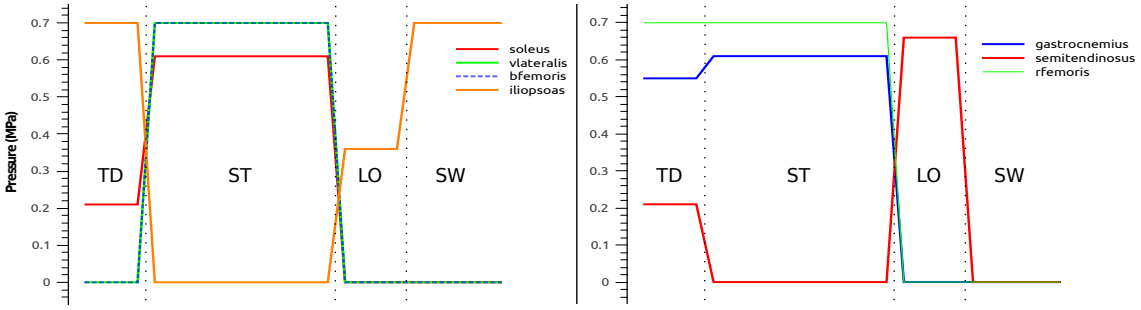

Figure 4.5: Activation pattern for the hindlimbs. On the left inset we have monoarticular muscles, while on the right one biarticular muscles are depicted. The four phases of the gait (TD, ST, LO and SW) are defined as touch down, stance, lift off and swing, respectively.

trol a fairly unexplored field.

While Maufroy[36] approaches unloading rule in uncoupled hindlimbs in his work, the lack of a musculoskeletal compliant structure inhibits it from observing muscular contribution to stability or a deeper study on joint angles and force sensors during such compliant locomotion. Our study simulates muscles, considering compliance during gait and EMG-based muscular activation, mimicking animal locomotion to a higher extent than the former, which used pre-defined trajectories on non-compliant electric motors attached to limb joints.

Differently from Ekeberg's simulation, we used a force sensor on each hindlimb, instead of soleus muscular tension, as ground force measuring method. The force sensing resistor (Interlink Electronics, FSR408) was tuned, specially considering the sensor's precision, degraded by deformable materials on the tip of the hindlimb.

Preliminary experiments with pressure sensors on the soleus muscle have shown that during stance phase the noise created while activating other muscles resulted in accidental triggering of the unloading rule. The addition of a low-pass filter degraded the system response, and other equally sensitive alternatives (such as strain gauges) are likely to suffer from the same shortcoming. In the future, we will adopt a muscle tension measuring alternative to better reproduce this biological idea.

4.3 Experiments

Experiments were conducted in a controlled environment, with a treadmill running at constant speed (0.8 km h^{-1}) and a tether connected to the robot, supplying energy (12 V), compressed air (0.6 MPa) and exchanging robot attitude data with a computer (muscle pressure, force sensor signal). With the sole purpose of understanding and reproducing feline locomotion on a treadmill, no special attention was paid to energy efficiency, air consumption or remote applications.

The treadmill speed was defined after trials with the robot, being the chosen speed the robot's baseline speed. Initially, Ekeberg's adopted activation pattern[14] and EMG signals were compared, creating an activation pattern inspired on these levels. As this pattern did not create a stable walking, joint angles from videos with walking cats were compared with observed values and specific muscles were tuned at 0.2 bar increments until a roughly stable walking was possible. From this point, an iterative process started, tuning force sensor thresholds and muscle activation pattern to reach the most stable walking, thus called baseline. Aiming to validate the unloading rule on such morphology this trial and error method was chosen over optimization algorithms due to the vast data on cats locomotion, angles and time constraints, where other methods could have created other locomotion gaits, outside of our research scope.

The experiments were conducted in two different experimental settings: a first experiment aimed to understand individual contributions from muscles on the gait stability during cat stepping, while the second introduced obstacles to see what influence it had on the robot rhythmic stability. Both experiments adopted the unloading rule as an alternating phase attractor state, as suggested by Ekeberg[14], and aim to prove that this rule is adaptive enough to withstand morphological (muscle pressure) and environmental (obstacles) changes in a real world experiment, while Ekeberg only considered environmental changes.

As a stability measuring criteria, we registered the influence of these disturbances on the phase difference between right and left hindlimbs. Similarly to Ekeberg, the phase difference is defined by:

$$\Phi_{H(actual)} = \frac{T_{H(actual)} - T_{O(previous)}}{T_{O(next)} - T_{O(previous)}}$$

where Φ_H is the specified hindlimb's phase, H and O standing for hindlimb and opposite hindlimb and T standing for the moment in which the hindlimb touches the floor. The idea is that the phase of each hindlimb is defined in association with the floor touching moments of the opposite hindlimb.

While the robot walks on the treadmill, many methods for acquiring data were used: the microcontroller which controls the robot sends attitude serial data to a computer, and on the outside a motion capture system is used to acquire data pertaining to the robot's position, speed and angles.

4.3.1 Experimental Method

The experiment starts by placing the robot on the running treadmill. When the hindlimbs, which are in Touch down phase, touch the treadmill, walking starts naturally. The parameter being tested is set prior to the experiment, adopting the baseline with one variable value, which might be muscular pressure or force sensor threshold, and 20 steps are recorded on the motion capture system. When a stable walking is not possible, with the robot falling before 20 steps, the experiment is labeled as a fail and halted. Second and third trials of unsuccessful experiments didn't result in a success, usually collapsing before reaching a stable 10th step.

Although in the majority of the success cases more than 40 steps were possible, only 20 recorded steps are plotted, with no observable stability difference between the recorded and unrecorded experiments. Falling after long time stable walking happened by the robot falling through one of the extremities of the treadmill (too slow or too fast), breaking parts (many ABS plastic parts fatigued during experiments) or slippage (after starting the stance phase, the leg slips to the back, finishing stance before the opposite leg started it). Failed walking experiments usually happened by lack of muscle strength or incorrect hindlimb coordination.

On the second experiment, baseline parameters are used to measure the alternating gait stability when different obstacles are introduced on the treadmill. Initially, stable gait is produced and then the

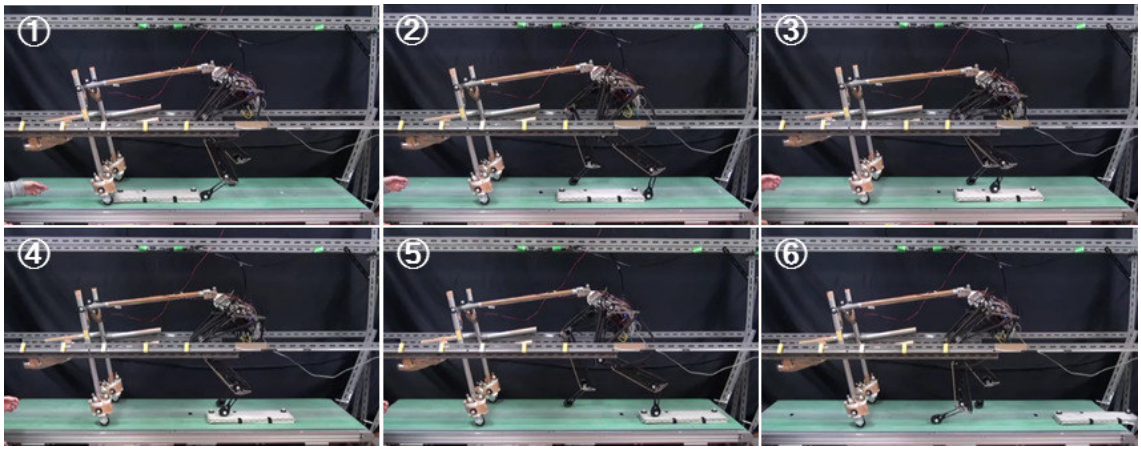

Figure 4.6: Walking experiment with hindlimbs attached to moving structure, passing through an obstacle. From the top left to the top right an alternating gait with left stance and then right stance. In (3) the left leg touches the obstacle, initiating stance at (4), continuing the alternating gait afterwards.

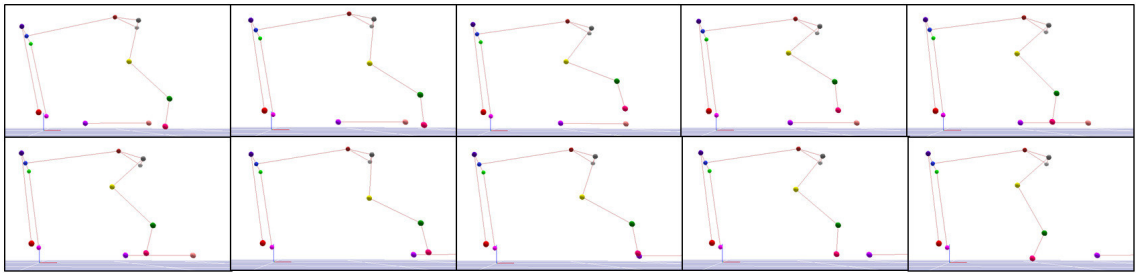

Figure 4.7: Walking experiment with an obstacle, recorded by a motion capture system. Markers attached to the left hindlimb show it overcoming an obstacle, extracted from Fig. 4.6. Movement progresses from top left corner to top right corner, and then from bottom left to bottom right.

obstacle is introduced on the treadmill. Experiments are labeled as a success if 6 steps are produced after the obstacle was passed. All experiments labeled as success were capable of continuing walking after 6 steps, but we restricted the plotted data to 6 steps to focus on the gait disturbance phenomenon (being 3 steps on each leg enough to bring the system back to steady state). In Fig. 4.6 and 4.7 the robot overcoming an obstacle on the treadmill is shown from a video camera and a motion capture system, respectively.

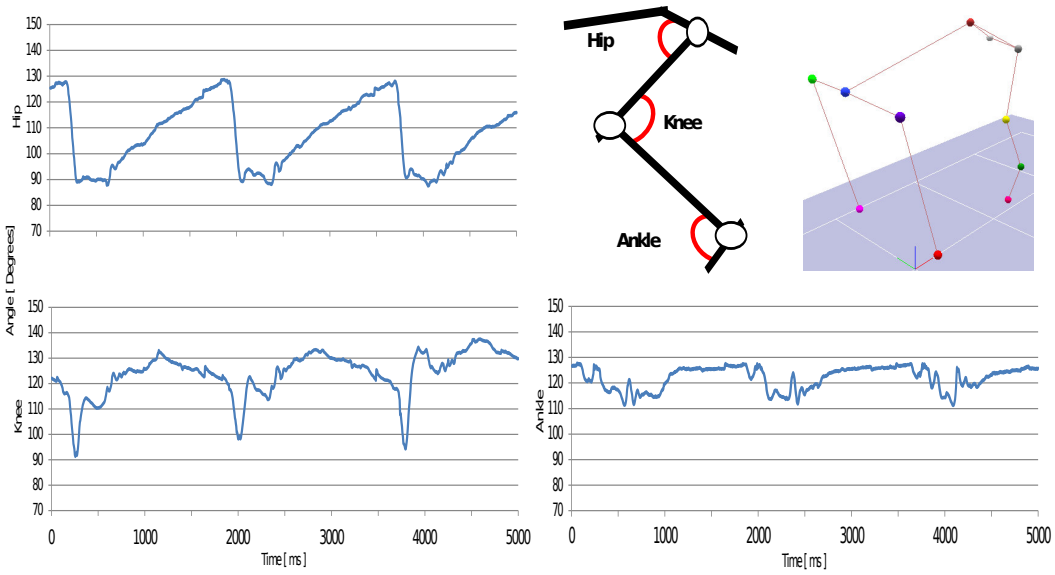

Figure 4.8: Angular position of hip, knee and ankle during walking with baseline parameters.

4.4 Results

Initial trials allowed the reproduction of a stable walking on the treadmill, defining the baseline for the robot. In Fig. 4.8, knee, ankle and hip angles, extracted with motion capture, are shown during a stable walking on the treadmill. During stepping the angular range of motion for ankle, knee and hip are respectively $17°$, $50°$ and $40°$.

Focusing on swing and stance phases, Fig. 4.9 shows the behavior of the hindlimb during these two phases. The ground clearance produced during swing is of 40 mm, while the stride length is 450 mm. To prove that the alternating gait produced by the unloading rule is stable enough to overcome disturbances we proceeded to tests with different parameters.

4.4.1 Systematic changes on walking parameters

The influence on the alternating stability was initially tested with different threshold values at the ground reaction force sensors, as seen in Fig. 4.10, and later the same contribution was evaluated for

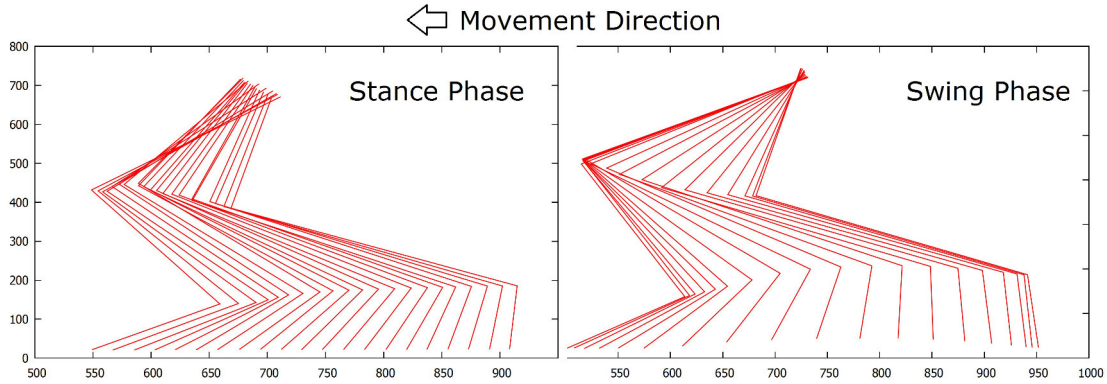

Figure 4.9: Digitized stance and swing phases recorded with a motion capture system with baseline parameters. Both stick figures are representative data, based on the mode of 20 steps, having a very low variability between steps. X and Y axis are expressed in milimeters.

different pressures on gastrocnemius muscle during stance phase (Fig. 4.11). While small thresholds could still produce stable walking, bigger thresholds greatly decreased stability. For the gastrocnemius muscle, any pressure lower than 0.36N was insufficient to keep the robot standing during stance, while bigger pressures also degraded walking stability.

The next step consisted in analyzing contributions from different muscles. Alternating gait stability with the muscle rectus femoris during stance was evaluated, as seen in Fig. 4.12.

During walking rectus femoris proved to be essential for weight bearing, resulting in body collapse after a few steps whenever the pressure was lower than 0.3 MPa. Differently from gastrocnemius, an upper limit for rectus femoris stability during stance was not observed.

4.4.2 Systematic changes on walking environment

A second set of experiments used the baseline setting to measure influence of obstacles on gait stability. Initially we used a motion capture system to analyze the effects of an obstacle on joint angles during walking (similarly to previously shown Figures 4.6 and 4.7). In Fig. 4.13 we can see the hindlimb overcoming an obstacle, while in Fig. 4.14 the hip, knee and ankle joint angles from this experiment are shown.

Upon finishing touch down phase prematurely, the hindlimbs have to account for the height differ-

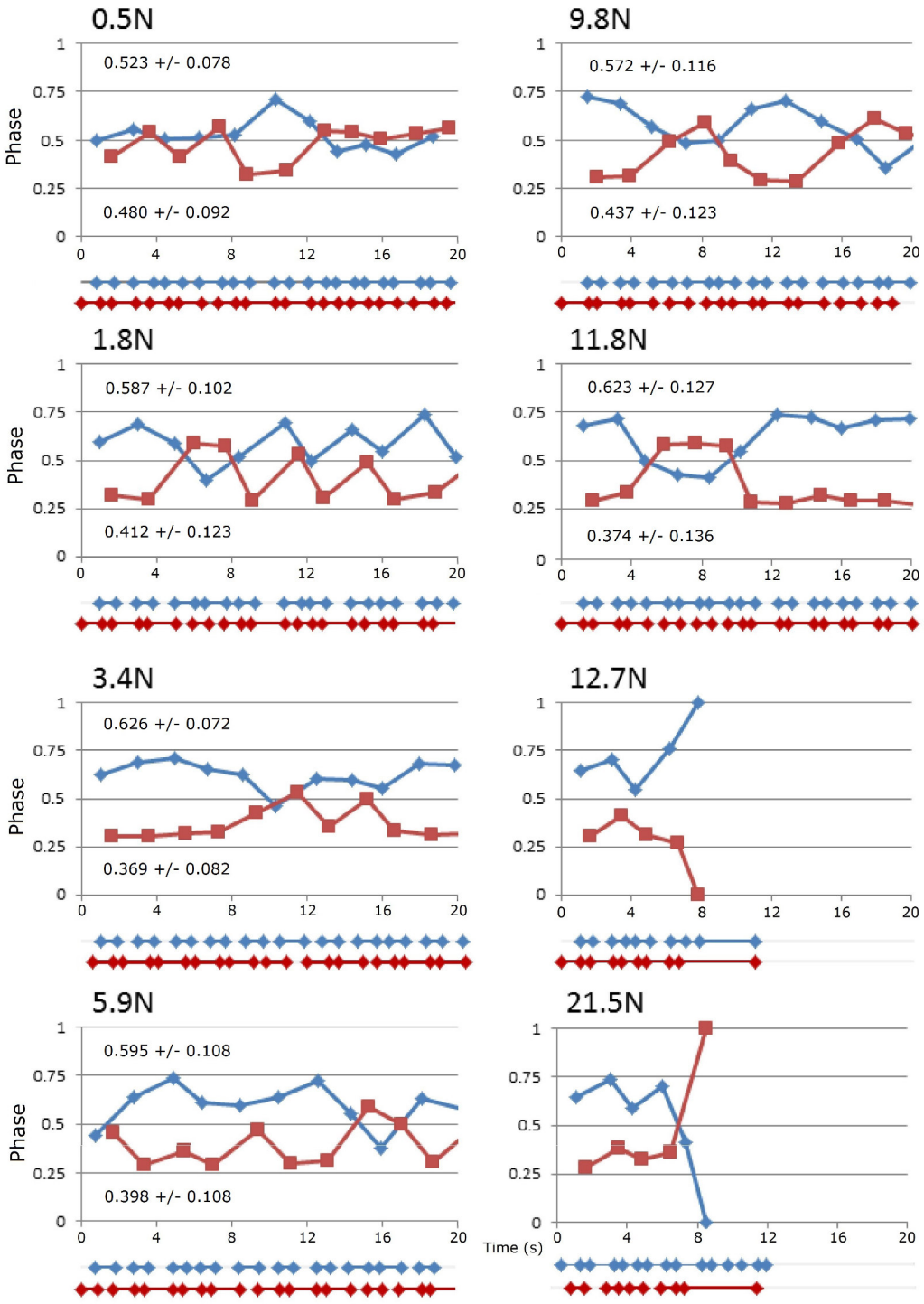

Figure 4.10: Contribution to alternating gait for different values of stance-to-swing threshold. Red lines represent right hindlimbs, blue lines represent left hindlimbs and their mean and standard deviation are depicted on each graph.

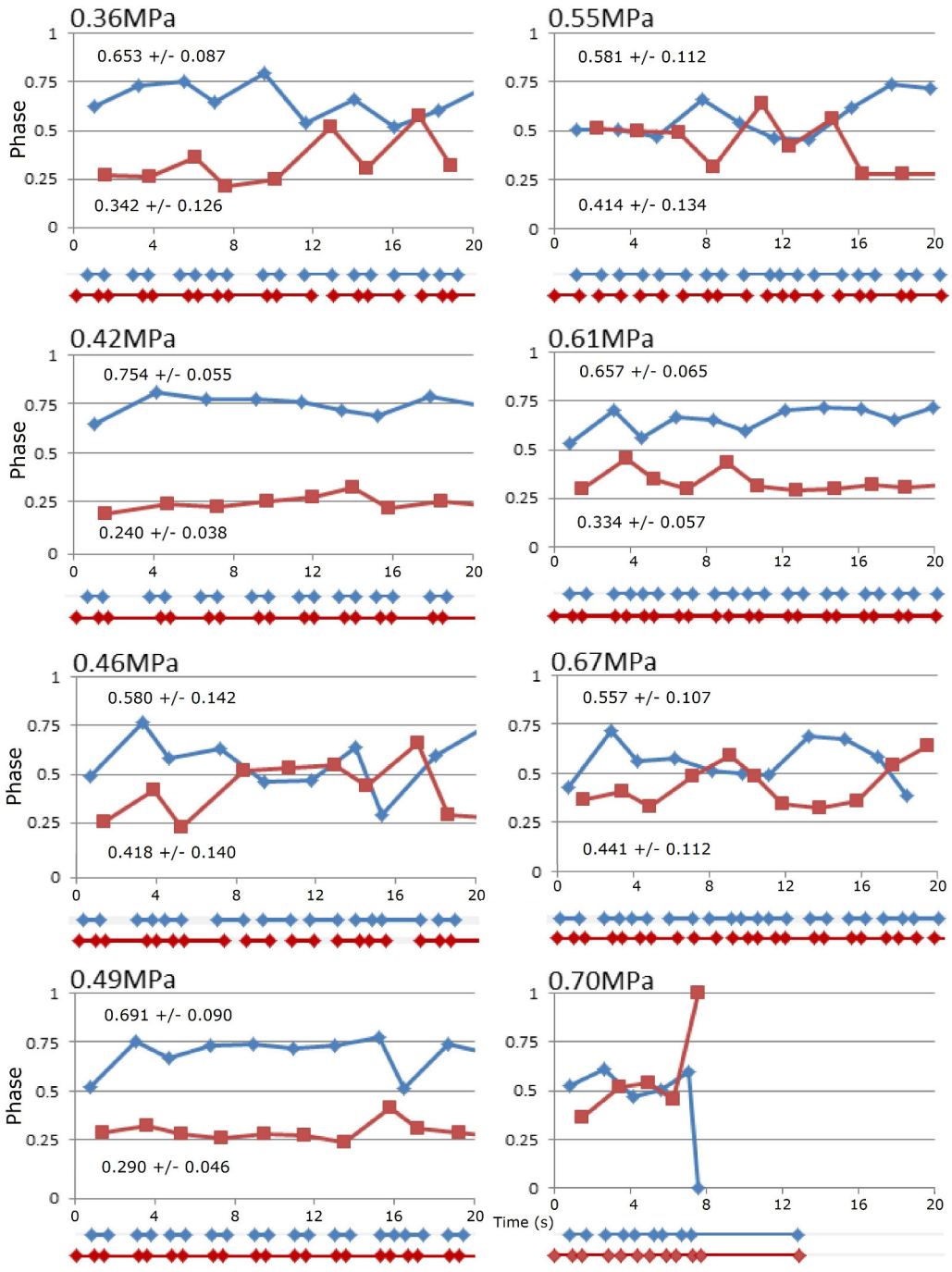

Figure 4.11: Contribution to alternating gait for different values of gastrocnemius pressure during stance. Red lines represent right hindlimbs, blue lines represent left hindlimbs and their mean and standard deviation are depicted on each graph.

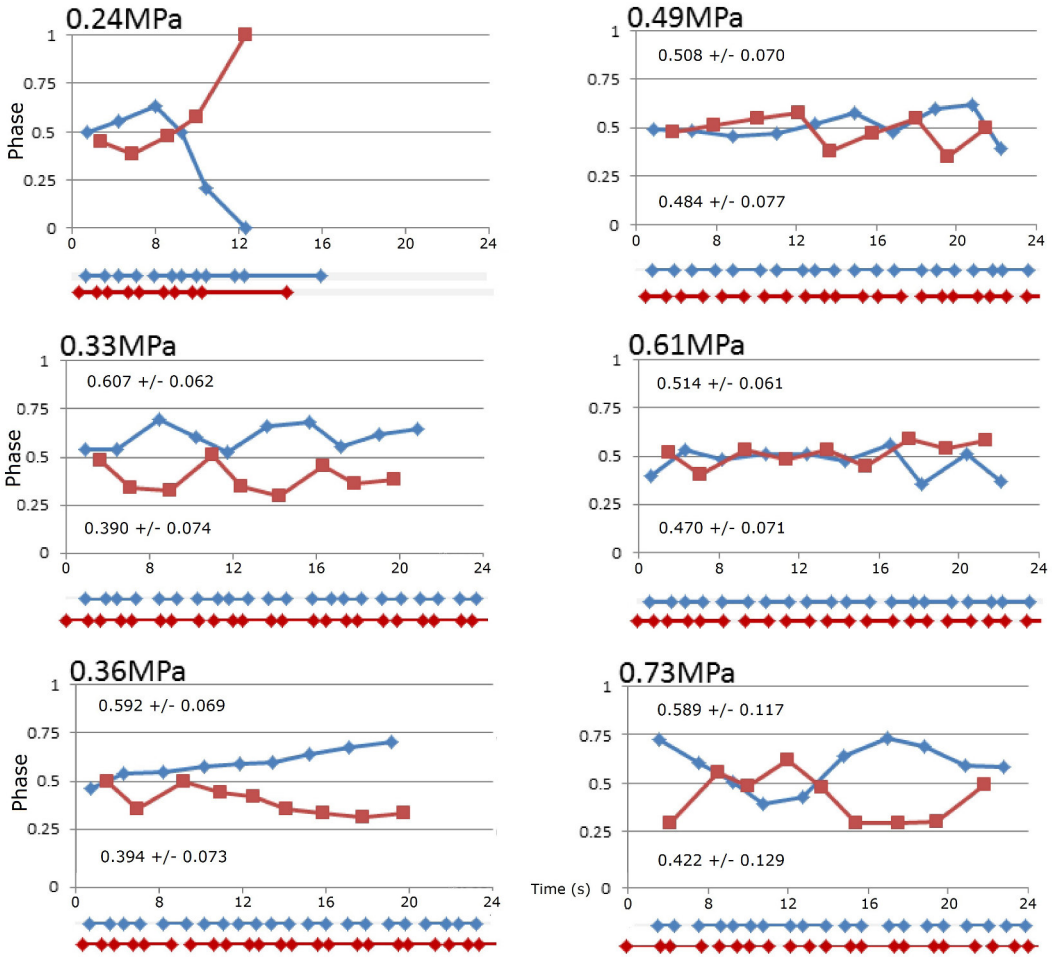

Figure 4.12: Contribution to alternating gait for different values of rectus femoris pressure during stance. Red lines represent right hindlimbs, blue lines represent left hindlimbs and their mean and standard deviation are depicted on each graph.

ence, with the effect being dealt at a morphological level (no change in the activation pattern), without compromising alternating gait. In Fig. 4.13 the knee (a) and ankle (b) joint behavior during disturbance is emphasized.

Finally, trials with obstacles of different heights were performed on the treadmill, registering the alternating gait stability while overcoming obstacles (Fig. 4.15). Although the robot could pass through 8 mm obstacles without major stability disturbances, bigger obstacles created bigger disturbances. With a gradually increasing height, eventually the robot was not capable of stabilizing after stepping on an

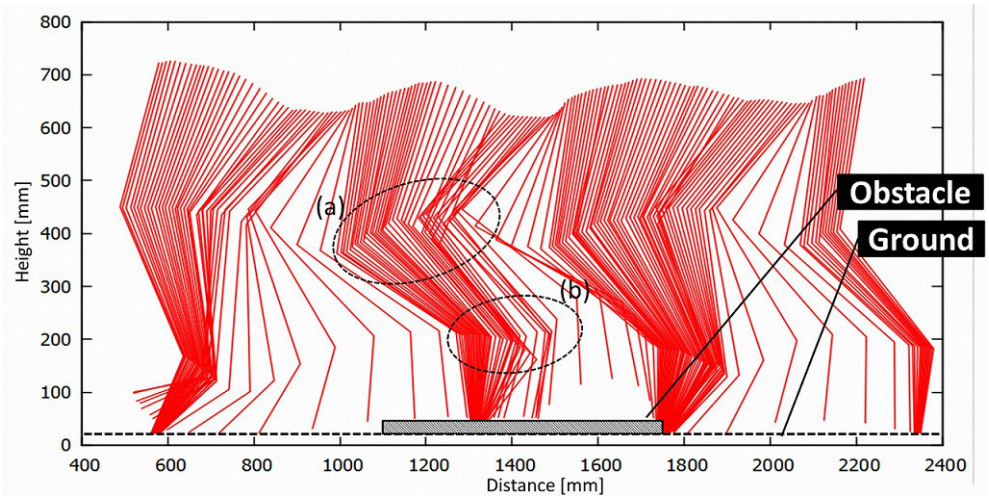

Figure 4.13: Influence of a 17.5 mm obstacle on the uncoupled alternating gait behavior. Upon finishing touch down phase prematurely, knee (a) and ankle (b) joints react differently to keep stability.

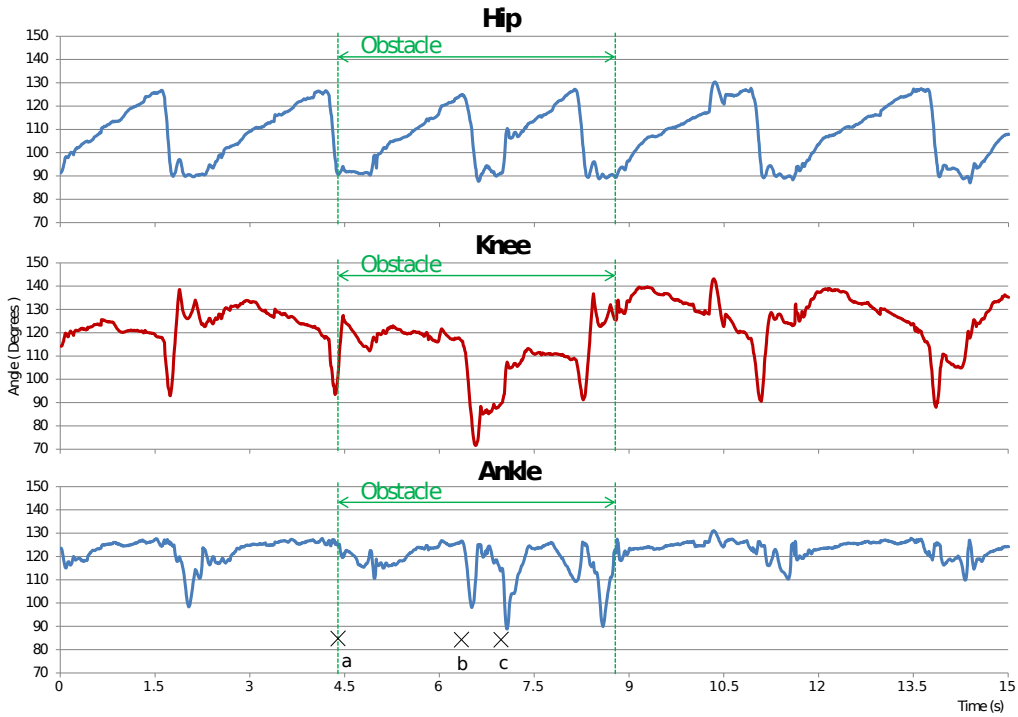

Figure 4.14: Influence on hip, knee and ankle joint angles of a 17.5 mm obstacle on the uncoupled alternating gait behavior.

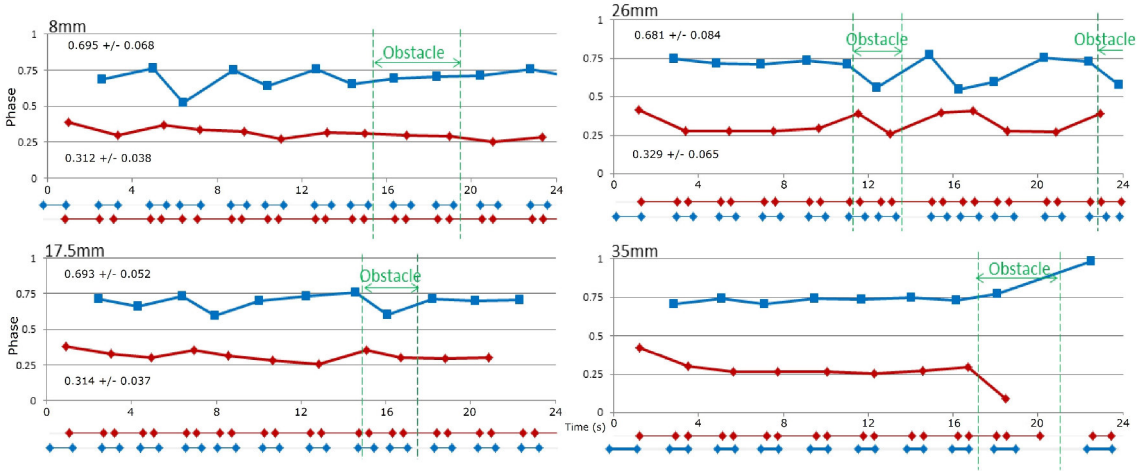

Figure 4.15: Trials with different obstacles, probing Pneupard's limits overcoming disturbances. Red lines represent right hindlimbs, blue lines represent left hindlimbs and their mean and standard deviation are depicted on each graph.

obstacle, collapsing at obstacles with 35 mm.

4.5 Discussion

4.5.1 Alternating gait through unloading rule

Inspired by findings from[14], where an alternating gait could be reproduced solely by using a bio-inspired unloading rule, we developed a real-life experiment with realistic moment arms and adopted the same rule. With the intent to assess if such rule would be capable of generating an alternating gait, initial trials were performed, tuning muscles and sensors. After some tests, the walking gait presented a natural alternating behavior, which prevented the robot from entering a bounding gait condition.

Comparing hip, knee and ankle angles from Fig. 4.8 to angles extracted from unrestrained animals[23], the three curves from the robot resemble the biological curves, with two noticeable differences: First, the biological ankle range of motion is 30°, which is more than that observed on the robot (17°). Second, the hip swing angular speed on the robot is faster than values observed on cats (steep hip curve pointing downwards in Fig. 4.8). Although these differences are not really associated with the unloading rule *per se*, they may imply that even though the movement was slightly unnatural, the attractor

state created by the unloading rule compensated for these differences. We believe that further tuning on the baseline parameters to reproduce a more compliant ankle joint and a smoother swing would make the robot behavior more animal-like.

While in Ekeberg[14] a symmetric gait is observable during unloading rule, the same was not true in our experiments. While in computational environments reproducing perfectly symmetric legs is possible, the errors involved in the artificial muscle construction collaborated to different muscular lengths between legs. Our experiments had a stable gait with one hindlimb's phase at 0.7 and the other at 0.3, meaning that contracted muscles made one look shorter than the other, even though both have exactly the same length (both hindlimbs were made in high precision equipments, such as industrial grade CNC and fused deposit modeling 3D printer). One more time, the fact that the stability was maintained amidst assymetric construction fortifies the hypothesis that the attractor state created by the unloading rule is strong enough to overcome systematic disturbances.

In Fig. 4.10 different threshold values were used, resulting in stable gait up to a threshold value of 11.8N. Since stance-to-lift off thresholds are reached when the ground reaction force naturally decreases, higher thresholds forced the robot to shift to lift off before the stance was supposed to finish. In many such occasions, the stance phase was so short that the opposite hindlimb was still in swing, creating a flight phase, which was not supposed to be observed in walking. Consequently, with the opposite hindlimb landing in swing phase (with a different attack angle than the one observed in touch down) the robot collapses.

4.5.2 Muscular contribution to alternating gait

The muscular activation pattern developed during trials served as a template to be repeated, being the unloading rule the trigger for phase changes. Among 7 active muscles used during this experiment, only gastrocnemius and rectus femoris were chosen as variable parameters. The main reason for this choice is that gastrocnemius and rectus femoris are, among with soleus, vastus and biceps femoris, the major weight bearers in animals. Focusing on an ankle extensor and a knee extensor allowed us

to see different effects on walking. Future works with this same platform will investigate synergistic contribution from other muscles on a walking experiment.

In Fig. 4.11 experiments with gastrocnemius muscle were shown. Two collapsing situations were clearly depicted: Low gastrocnemius pressure and high gastrocnemius pressure. For the first case, decreasing the amount of force done by gastrocnemius passes the extra burden to soleus, which[29] proved to be more than 4 times smaller than gastrocnemius in a cheetah. This way the robot collapses for lack of ankle stiffness, standing in a 2-link position (plantigrade) instead of a 3-link (digitigrade). The second case results in an overstiff muscle, locking the ankle joint at $130°$, not complying when touching the floor. The angle of $130°$ was set as a maximum value with a hard mechanical stop for walking experiments. Apparently, compliance plays a very important role on ankle joint, where an overcompliant or overstiff ankle affects stability negatively.

In Fig. 4.12 rectus femoris contribution to stability was measured. Although a lower limit for stability could be observed, there was no maximum pressure which could degrade walking stability. All experiments with pressure below 0.3MPa eventually collapsed the robot for lack of knee joint stiffness, where the muscle vastus lateralis was eventually trying to keep the robot standing on its own. Best stability results were found with muscle pressure between 0.49MPa and 0.61MPa, where we assume that an optimal knee compliance was achieved.

4.5.3 Obstacle influence on alternating gait

Changing the walking environment has a negative effect on biological gait, which is shortening the swing/touch down cycle. In Figures 4.13 and 4.14 the hindlimb passes through a 17.5 mm obstacle and hip, knee and ankle joints angles are registered during the experiment. As seen on Fig. 4.13 the first contact with the obstacle happens while leaving lift off phase to swing, "kicking" the obstacle (marked with (a) in Fig. 4.14). This disturbance affects the knee and ankle angles, generating an abnormal swing phase, and has no effect on hip angle (this first disturbance is represented as the first half of the period marked as obstacle in Fig. 4.14). Upon touching the obstacle instead of the floor, the joints have to

compensate the height difference with the muscular compliance provided by the artificial muscles. During this condition, the ankle which was usually in phase with the other 2 joints bends faster upon touching the obstacle (b), slipping and touching it for a second time (c), reaching a stance position with abnormal behavior and proceeding to swing again (last spike inside obstacle mark).

The same disturbances affect the knee joint in a different way. While "kicking" the obstacle, knee joints behave as if angles were offset in $-10°$, decreasing as a whole during the first half of the obstacle mark in Fig. 4.14. In the second half, where slippage and stance in obstacle happens, knee angles are offset even more to compensate for the different height, returning to normal behavior right after the obstacle is passed. Similarly to observations from gastrocnemius/rectus femoris muscles, the knee joint seems more stable than the ankle joint, being the hip joint the least susceptible to disturbances of all. While distal joints are more prone to high frequency disturbances, proximal joints only feel low frequency one, being the knee in the medium frequency range.

The presence of a strong state attractor on the unloading rule was enough to overcome obstacles on the treadmill, as shown in Fig. 4.15. Nevertheless, obstacles with 35 mm and beyond could not be dealt with this simple rule. When passing through smaller obstacles, the transition from swing to touch down phase occur in midair, cancelling leg flexion forces and preparing the leg for landing, where sensory feedback will start the stance phase. We believe that there were mainly two falling conditions:

1. Although the floor clearance from the robot is 40 mm, this value is only true at the middle of the swing phase, with smaller values in the beginning and end of swing. This condition results in obvious consequences, with the robot stumbling on the obstacle, with a possible solution being an improved ground clearance.

2. The negative influence on the opposite leg when the hindlimb touches the obstacle without transitioning from swing to touch down phases. This condition is less obvious, and better explained by the unloading rule itself: When the ground reaction force decreases below a threshold, the hindlimb finishes stance phase. This means that when an unprepared hindlimb touches the floor and does not enter stance phase, the small transfer of ground reaction force to this

hindlimb may accelerate the opposite hindlimb transition, resulting in both limbs at swing at the same time. This condition is specific to the algorithm used by the robot, where no sensing occurs during swing to avoid noise, being non-existent in biological systems.

4.6 Conclusion

In this work we investigated the alternating gait of feline uncoupled hindlimbs through the unloading rule. Using Pneupard as a test platform, we tried to physically reproduce biological phenomena hitherto hypothesized by biologists and simulated by scientists.

Initially, the design process for the biomimetic robot is explained, considering limb dimensions, important muscles and realistic moment arms. Comparisons between biological and artificial muscles are established and the EMG-based muscular activation pattern is presented. A finite state control is proposed, using the unloading of ground reaction force to transit from stance to lift off phase, having no coupling between right and left hindlimb. Before experiments it is verified that the coupling between hindlimbs is not needed and Pneupard is capable of a stable alternating gait on the treadmill with this simple biological rule.

Experiments analyze the contribution of individual muscles (rectus femoris and gastrocnemius) to the alternating gait, and different force thresholds to perform stance-to-swing transition are verified. The ability to overcome obstacles with different heights is tested and the robot is capable of keeping alternating stability against different disturbances while powered by the unloading rule.

As future outcomes of this research we could mention a better understanding of felines, explaining decerebrate walking and muscular roles during stepping. A deeper knowledge on animal locomotion would finally allow us to replicate it. From a robotic side, reproducing animal locomotion, which surpasses robotic performance in so many different ways, would lead to highly adaptive behavior in legged robots, increasing the range of applications to robots in society.

5

Conclusion

The main topic of this thesis is to understand the contribution from muscles to locomotion stability. Although brain and spine contributions were partially ignored in this work, they are also extremely important to locomotion, being the main focus of the majority of locomotion-related studies.

Upon focusing on muscles, their reaction at floor contact and their relationship within complex musculoskeletal limbs, a few observations emerged. Contributions from these experiments to biology and robotics will be first discussed, followed by the future of artificial muscles in robotics, and being concluded by future works to be performed in this area.

5.1 Study limitations

As any experiment where biological conditions are recreated artificially, our experiments had some study limitations. Air muscles are considered, so far, the best replacement for biological muscles in biomimetic robots, but they do not behave as biological muscles (specially when force-velocity relationship is considered). During hopping, muscle contraction rate is high (higher than walking), meaning that the forces exerted by our air muscles will be different than a similar biological muscle in this conditions. Moreover, the time to reach peak force in pneumatic muscles is higher than biological ones, creating a slower reaction time when "reflex" is being considered.

In Chapter 2 the proposed biomimetic hindlimb uses a vertical jump as a testing method. The author understands that biological locomotion is more complex than this vertical movement, merely functioning as a simplified experiment to test the leg.

The unloading rule in animals use muscular unloading, which takes into consideration not only ground reaction forces, but also variating moment arms at the ankle joint. Our approach in Chapter 4 only considered the former, not fully representing the biomechanical reality. Even though such approach may be considered as a simplification of the biological structure, it was faithful enough to reproduce observed phenomena. Further studies will take into account the variable moment arm at the ankle by measuring the force between muscle and structure.

Robotic asymmetry was mentioned in Chapters 3 and 4, with some phenomena being observed on one side and not holding true for the other. We believe that a perfectly symmetrical robot could have reproduced phenomena equally for both sides, but that is not the purpose of this work. The presence of asymmetry is not a limitation *per se*, specially when such feature is also present in humans and other bipeds. Instead of facing asymmetric data (non-significant to one side, significant to the other) as a failed experiment, we believe that this should be understood as an additional source of disturbance on the hopping system, common in real life experiments.

In all experiments parameters were tuned to achieve a performance as close as possible to the biological one. With the continuously changing conditions within the robot's body (mechanical strain on

joints and muscles while walking or jumping, leading to replacement of actuators and bearings), some fluctuation existed. Experiments were organized trying to minimize such errors, and had to be repeated whenever required.

5.2 Possible contributions to biology and robotics

Beyond simple actuators, muscles perform different roles on animal locomotion: they can purely behave as springs[1], storing potential elastic energy, or as pure dampers[13], reducing hopping amplitude. Moreover, with sensors embedded (muscle spindles), they are also capable of reacting quickly to disturbances and ground unevenness.

During experiments with a hopping biped (Chapter 2), the statistical insignificance present between delayed and non-delayed reflex responses makes clear the importance of such compliant structures. With evolving technology, unexpensive microcontrollers reach the amazing frequency of 100 MHz (e.g., Arduino Due), while a hopping human, with a 33 milliseconds delay between touch and activation[65], would have a "processing power" of 30Hz. Still, a comparison between a 5-years-old and any robot developed so far would be unfair when it comes to locomotion performance.

Apparently, the gap between robotic and animal "processing power" is filled and surpassed by the presence of muscles. More specifically, a combination of highly compliant materials with intricate inter-muscular rules. Beyond creating materials which behave exactly like muscles, the next step for biology and robotics in this field is to decode these very basic, "hardcoded" rules. As an example of such *basal rules*, the unloading rule, proposed by Pearson and Ekeberg[14,43], creates an alternating and stable walking gait just by enforcing a stance-to-swing transition when a specific threshold is reached. Another good example of such basal rules would be the stretch reflex. Hardcoded in every living being with muscles, every limb applies a contrary force when an external force is applied upon them.

Thus, with the main core of locomotion written within compliant muscles, this work helps both biological and robotic fields from a novel approach.

5.3 Future of muscles in robotics

Throughout this thesis the benefits from PAM are mentioned, being currently the closest actuator to biological muscles. Although these claims are true, the future pneumatic muscles on robotics is not promissing.

As a muscle replacement, artificial muscles should possess the compliance and controllability of muscles, allowing them to study and replicate basal rules. During hopping and walking experiments from this thesis, both criteria were met for indoor experiments, being the same performance hard to achieve in remote applications, outdoor. As stated by Wisse[67] and van der Linde[62], many ”benefits” from PAM vanish with remote applications: the high power-to-weight ratio decreases drastically when compressors, air tanks and regulators are added to the robot, the low cost of the muscle increases when the high cost of the pneumatic valve is considered and the presence of a ”dead volume” on the muscle increases air consumption, decreasing efficiency.

So far, studies with twisted carbon nanotubes, electroactive polymers and shape-memory alloys have created other sources of artificial muscles, but these are either too weak, slow or breakable for robotic applications. Being batteries the current standard for energy storage, the most efficient actuator for robots should convert this energy directly into mechanical energy, without other conversions. The combination of electric motors with torsional springs could generate compliant behavior (similarly to Series Elastic Actuators), but installing such actuators in distal parts of legs would increase moment of inertia, reducing speed and increasing energy usage.

Being the source of locomotion a combination of basal rules with compliant actuators, PAMs are the best choice for biomimetic studies within tethered environments with prototyped robots. From such actuators, a better grasp of the basal rules for locomotion can be obtained, and future applications on robots shall have other actuators, with some compliance, exploiting such rules to perform adaptive locomotion.

5.4 Future directions

In order to understand the basal rules governing locomotion, biomimetic research shall continue using artificial muscles, exploiting their compliance. Brain and spinal cord are already vastly approached by other roboticists, but rarely seen in compliant structures, like musculoskeletal systems. To reach a higher level of stability and adaptability, *muscles alone may not be enough*, but a future combination with other bio-inspired control methods might bring robots closer to biological behavior.

Recently developed, CPG is a very prominent control alternative which uses bio-inspiration to create movements. Similarly to a spinal cord, this controller emits rhythmic feed-forward outputs which activates actuators to perform cyclic movements, such as hopping, walking or running. An integration of such method with PAM, while adopting other basal rules (unloading, stretch reflex, etc.), will not only lead to a stable gait, but will also allow changing gaits, which is another unexplored area for legged robotics.

Future robots will probably not use linear muscles, opting for rotatory actuators instead, but insights absorbed from biomimetic experiments with muscles shall pave the way to stable legged robotics. In the long term, processing power advances shall be used to improve higher-level control, such as vision, human-interaction and artificial intelligence, cascading to the lower-level controller fewer parameters, instead of a fully fledged leg trajectory calculation (traditional approach).

In this vein, more researches trying to 1) understand the basal rules which lead to stable locomotion and 2) create alternative actuators which can efficiently replicate the compliance needed to perform adaptive locomotion should emerge.

A

Robot Design

A.1 Jumping biped

The construction of the robot involved a milling machine (MDX-540, Roland Corporation) and a 3d Printer (Connex260, Objet Geometries Ltd.), among other hand-cut materials. A list of main specs can be found in Table A.1. The construction aimed to mimic the musculoskeletal structure of human beings, including maximum moment arms (Fig. A.1).

Touch sensors were made by using force-sensing resistors (FSR-406, Interlink Electronics) with a 7.5 kΩ resistor, with the chosen touch threshold being 1.2 V. The adopted pneumatic valves (VQZ1321,

Table A.1: Jumping Robot specs

Parameter	Value
Shoulder-Hip Distance	630mm
Hip-Knee Distance	360mm
Knee-Ankle Distance	340mm
Inter-feet Distance	200mm
COG height	780mm
Weight	7.8 kg
Hip range of motion	$-45°$~$90°$
Knee range of motion	$-120°$~$0°$
Ankle range of motion	$-60°$~$60°$
Air muscle contraction rate	30%
Air muscle length	200mm

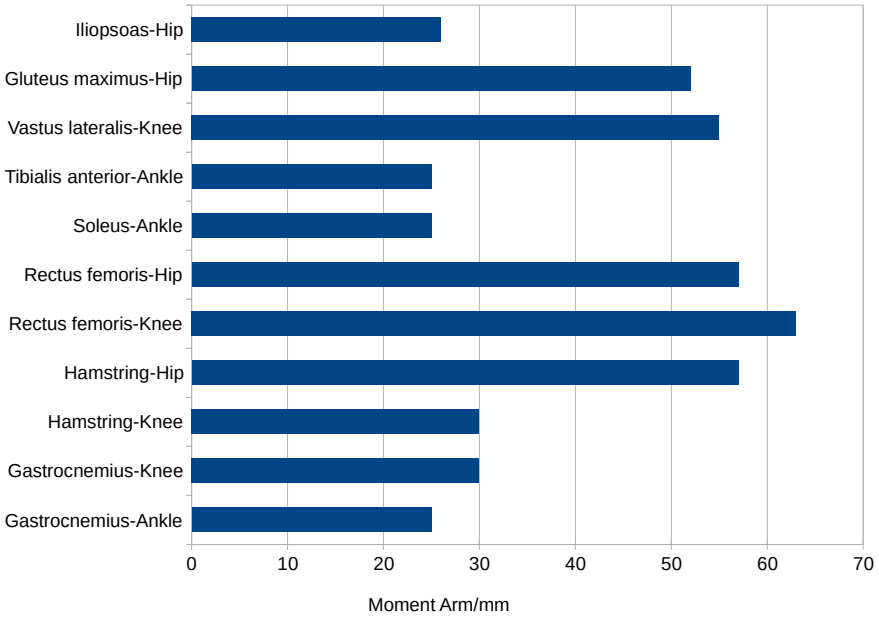

Figure A.1: Graph with maximum moment arms used during robot construction.

SMC Corporation) connect to the muscles, having a pressure sensor (PSE540, SMC Corporation) connected between them. All the valves exhaust to the room and are supplied by a compressor (2000-40m, Jun Air) through a tether. A 3 DOF accelerometer (KXR94, Kionix Inc.) and 2 gyroscopes (CRS03, Silicon Sensing Systems) are combined in a complementary filter to generate roll and pitch angle infor-

mation.

The complementary filter adopted to register roll angle during jumping used gyroscope (1 axis) and accelerometer (2 axis) to create an estimation of roll angle. Initially, both Y and Z axis of the accelerometer were used to find an angular projection in the frontal plane, using:

$$\Theta_{a(x,n)} = arctan(y/z)$$

where y and z are the coordinates of the force vector registered by the accelerometer and $\Theta_{a(x)}$ is the angular position around the X axis, according to accelerometer at instant n. The gyroscope, on the other hand, registers angular velocity, and thus uses a previous angular estimation to update itself:

$$\Theta_{g(x,n)} = \Theta_{e(x,n-1)} + \dot{\Theta}_{g(x,n)} T$$

where T is the sample period. This way, with both contributions from accelerometer and gyroscope, the new estimate is calculated:

$$\Theta_{e(x,n)} = \frac{\Theta_{a(x,n)} + w\Theta_{g(x,n)}}{1 + w}$$

where w is the weight, which in this case was 90.

References

[1] Alexander, R. (1995). Leg design and jumping technique for humans, other vertebrates and insects. *Phil. Trans. R. Soc. Lond. B.*, 347, 235–248.

[2] Anthony, D. A. (2007). *The horse, the wheel, and language: how Bronze-Age riders from the Eurasian steppes shaped the modern world*. Princeton University Press.

[3] Aschenbeck, K., Kern, N., Bachmann, R., & Quinn, R. (2006). Design of a quadruped robot driven by air muscles. In *IEEE Intl. Conf. Biomed. Robot. and Biomechatronics* (pp. 875–880).

[4] Azizi, E. & Roberts, T. (2013). Variable gearing in a biologically inspired pneumatic actuator array. *Bioinsp. Biomim.*, 8, 026002.

[5] Bertsekas, D. & Tsitsiklis, J. (1995). Neuro-dynamic programming: an overview. In *IEEE Intl. Conf. Decision and Control* (pp. 560–564).

[6] Boblan, I., Bannasch, R., Schewenk, H., Prietzel, F., Miertsch, L., & Schulz, A. (2004). *Embodied Artificial Intelligence*, chapter A human-like robot hand and arm with fluidic muscles: biologically inspired construction and functionality, (pp. 160–179). Springer Verlag.

[7] Brown, T. (1911). The intrinsic factors in the act of progression in the mammal. *Proc. Roy. Soc. B*, 84, 308–319.

[8] Burkholder, T. & Nichols, T. (2004). Three-dimensional model of the feline hindlimb. *J. Morphol.*, 261, 118–129.

[9] Calisti, M., Giorelli, M., Levy, G., Mazzolai, B., Hochner, B., Laschi, C., & Dario, P. (2011). An octopus-bioinspired solution to movement and manipulation for soft robots. *Bioinsp. Biomim.*, 6, 036002.

[10] Carpenter, M., Allum, J., & Honegger, F. (1999). Directional sensitivity of stretch reflexes and balance corrections for normal subjects in the roll and pitch planes. *Exp. Brain Res.*, 129, 93–113.

[11] Day, L. & Jayne, B. (2007). Interspecific scaling of the morphology and posture of the limbs during locomotion of cats (felidae). *J. Exp. Biol.*, 210, 642–654.

[12] Diamond, J. (1983). The biology of the wheel. *Nature*, 302(5909), 572–573.

[13] Dyhre-Poulsen, P., Simonsen, E., & Voigt, M. (1991). Dynamic control of muscle stiffness and h reflex modulation during hopping and jumping in man. *J. Physiol.*, 437, 287–304.

[14] Ekeberg, O. & Pearson, K. (2005). Computer simulation of stepping in the hind legs of the cat: an examination of mechanisms regulating the stance-to-swing transition. *J. Neurophysiol.*, 94, 4256–4268.

[15] Engberg, I. & Lundberg, A. (1969). An electromyographic analysis of muscular activity in the hindlimb of the cat during unrestrained locomotion. *Acta Physiol. Scand.*, 75, 614–630.

[16] English, A. (1978). An electromyographic analysis of forelimb muscles during overground stepping in the cat. *J. Exp. Biol.*, 76, 105–122.

[17] Fallon, J., Bent, L., McNulty, P., & Macefield, V. (2005). Neuromechanical models for insect locomotion: Stability, maneuverability, and proprioceptive feedback. *J. Neurophysiol.*, 94, 3795–3804.

[18] Fibley, R. & Gazzaniga, M. (1969). Splitting the normal brain with reaction time. *Psychonomic Science*, 17, 335–336.

[19] Fukuoka, Y., Kimura, H., & Cohen, A. (2003). Adaptive dynamic walking of a quadruped robot on irregular terrain based on biological concepts. *J. Robot. Res.*, 22, 187–202.

[20] Full, R., Earls, K., Wong, M., & Caldwell, R. (1993). Locomotion like a wheel? *Nature*, 365(495), 495.

[21] Geyer, H., Seyfarth, A., & Blickhan, R. (2003). Positive force feedback in bouncing gaits. *Proc. R. Soc. Lond. B*, 270, 2173–2183.

[22] Gielen, S., van Ingen Schenau, G., Tax, T., & Theeuwen, M. (1990). *Multiple Muscle Systems: Biomechanics and Movement Organization*, chapter The activation of mono- and bi-articular muscles in multi-joint movements, (pp. 302–311). Springer Verlag.

[23] Goslow Jr., G., Reinking, R., & Stuart, D. (1973). The cat step cycle: hind limb joint angles and muscle lengths during unrestrained locomotion. *J. Morphol.*, 141, 1–42.

[24] Haeufle, D., Grimmer, S., Kalveram, K., & Seyfarth, A. (2012). Integration of intrinsic muscle properties, feed-forward and feedback signals for generating and stabilizing hopping. *J. R. Soc. Interface*, 9, 1458–1469.

[25] Haeufle, D., Grimmer, S., & Seyfarth, A. (2010). The role of intrinsic muscle properties for stable hopping - stability is achieved by the force-velocity relation. *Bioinsp. Biomim.*, 5, 016004.

[26] Hiebert, G. & Pearson, K. (1999). Contribution of sensory feedback to the generation of extensor activity during walking in the decerebrate cat. *J. Neurophysiol.*, 81, 758–770.

[27] Hosoda, K., Sakaguchi, Y., Takayama, H., & Takuma, T. (2010). Pneumatic-driven jumping robot with anthropomorphic muscular skeleton structure. *Auton. Robot.*, 28, 307–316.

[28] Hudson, P., Corr, S., Payne-Davis, R., Clancy, S., Lane, E., & Wilson, A. (2011a). Functional anatomy of the cheetah (acinonyx jubatus) forelimb. *J. Anat.*, 218, 375–385.

[29] Hudson, P., Corr, S., Payne-Davis, R., Clancy, S., Lane, E., & Wilson, A. (2011b). Functional anatomy of the cheetah (acinonyx jubatus) hindlimb. *J. Anat.*, 218, 363–374.

[30] Hyon, S. (2002). Development of a biologically inspired hopping robot kenken. In *IEEE Intl. Conf. on Robotics and Automation* (pp. 3984–3991).

[31] Klute, G., Czerniecki, J., & Hannaford, B. (2002). Artificial muscles: Actuators for biorobotic systems. *Int. J. Robotics Res.*, 21, 295–309.

[32] Kukillaya, R., Proctor, J., & Holmes, P. (2009). Neuromechanical models for insect locomotion: Stability, maneuverability, and proprioceptive feedback. *Chaos*, 19, 026107.

[33] Lam, T. & Pearson, K. (2002). *Sensorimotor Control of Movement and Posture*, chapter The role of proprioceptive feedback in the regulation and adaptation of locomotor activity, (pp. 343–356). Kluwer Academic.

[34] Lewisy, M., Buntingy, M., Salemi, B., & Hoffmann, H. (2011). Toward ultra high speed locomotors: design and test of a cheetah robot hind limb. In *IEEE Intl. Conf. on Robotics and Automation* (pp. 1990–1996).

[35] Maie, H., Oida, Y., Kitabatake, Y., & Egawa, K. (2001). Effect of hopping tempo on stretch-reflex of function soleus muscle at landing phase. *Jpn. J. Phys. Fitness Sports Med.*, 50, 139–148.

[36] Maufroy, C., Nishikawa, T., & Kimura, H. (2010). Stable dynamic walking of a quadruped robot kotetsu using phase modulations based on leg loading/unloading. In *IEEE Int. Conf. on Intelligent Robots and Systems* (pp. 5225–5230).

[37] McGeer, T. (1990). Passive dynamic walking. *Intern. J. Robot. Res.*, 9(2), 62–82.

[38] Melvil Jones, G. & Watt, D. (1971). Observations on the control of stepping and hopping movements in man. *J. Physiol.*, 219, 709–727.

[39] Modesto, S., Smith, R., Campione, N., & Reisz, R. (2011). The last "pelycosaur": a varanopid synapsid from the pristerognathus assemblage zone, middle permian of south africa. *Naturwissenschaften*, 98(12), 1027–1034.

[40] Muybridge, R. (1888). *Animal locomotion*. PhD thesis, University of Pennsylvania.

[41] Niiyama, R., Nishikawa, S., & Kuniyoshi, Y. (2010). Athlete robot with applied human muscle activation patterns for bipedal running. In *IEEE Intl. Conf. on Humanoids Robots* (pp. 498–503).

[42] Paul, C., Belloti, M., Jezernik, S., & Curt, A. (1969). Development of a human neuro-musculoskeletal model for investigation of spinal cord injury. *Biol. Cybern.*, 93, 153–170.

[43] Pearson, K., Ekeberg, O., & Buschges, A. (2006). Assessing sensory function in locomotor systems using neuro-mechanical simulations. *Trends in Neurosciences*, 29, 625–630.

[44] Perreault, E., Heckman, C., & Sandercock, T. (2003). Hill muscle model errors during movement are greatest within the physiologically relevant range of motor unit firing rates. *J.Biomech.*, 36, 211–218.

[45] Pfeifer, R. & Bongard, J. (2006). *How the body shapes the way we think*. MIT Press.

[46] Philippson, M. (1905). *L'autonomie et la centralisation dans le systeme nerveux des animaux. Trav. Lab. Physiol. Inst. Solvay*, 7, 1–208.

[47] Pierotti, D., Roy, R., Gregor, R., & Edgerton, V. (1989). Electromyographic activity of cat hindlimb flexors and extensors during locomotion at varying speeds and inclines. *Brain Res.*, 481, 57–66.

[48] Pratt, G. & Williamson, M. (1995). Series elastic actuators. In *IEEE Int. Conf. on Intelligent Robots and Systems* (pp. 399–406).

[49] Prilutsky, B., Herzog, W., & Allinger, T. (1996a). Mechanical power and work of cat soleus, gastrocnemius and plantaris muscle during locomotion: possible functional significance of muscle design and force patterns. *J. Exp. Biol.*, 199, 801–814.

[50] Prilutsky, B., Herzog, W., & Leonard, T. (1996b). Transfer of mechanical energy between ankle and knee joints by gastrocnemius and plantaris muscles during cat locomotion. *J. Biomech.*, 29, 391–403.

[51] Rasmussen, S., Chan, A., & Goslow Jr., G. (1978). The cat step cycle: electromyographic patterns for hindlimb muscles during posture and unrestrained locomotion. *J. Morphol.*, 155, 253–269.

[52] Romei, F. (2008). *Leonardo Da Vinci*. The Oliver Press.

[53] Rosendo, A., Liu, X., Shimizu, M., & Hosoda, K. (in press). Stretch reflex improves rolling stability during hopping of a decerebrate system. *Bioinspir. Biomim.*

[54] Rosendo, A., Nakatsu, S., Narioka, K., & Hosoda, K. (2013). Pneupard: A biomimetic musculoskeletal approach for a feline-inspired quadruped robot. In *IEEE Intl. Conf. Intelligent Robots and Systems* (pp. 1452–1457).

[55] Rosendo, A., Nakatsu, S., Narioka, K., & Hosoda, K. (2014). Producing alternating gait on uncoupled feline hindlimbs: muscular unloading rule on a biomimetic robot. *Advanced Robotics*, 28, 351–365.

[56] Rosendo, A., Narioka, K., & Hosoda, K. (2012). Muscle roles on directional change during hopping of a biomimetic feline hindlimb. In *IEEE Intl. Conf. on Robotics and Biomimetics* (pp. 1050–1055).

[57] Severin, F. (1970). The role of the gamma motor system in the activation of the extensor alpha motor neurones during controlled locomotion. *Biophysics*, 15, 1096–1102.

[58] Sinkjaer, T., Andersen, J., & B.Larsen (1996). Soleus stretch reflex modulation during gait in humans. *J. Neurophysiol.*, 76, 1112–1120.

[59] Sprowitz, A., Kuechler, L., Tuleu, A., Ajallooeian, M., D'Haene, M., Mockel, R., & Ijspeert, A. (2011). Oncilla robot : a light-weight bio-inspired quadruped robot for fast locomotion in rough terrain. In *5th Intl. Symp. Adaptive Motion on Animals and Machines* (pp. 63–64).

[60] Tsujita, K., Kobayashi, T., Inoura, T., & Masuda, T. (2008). Gait transition by tuning muscle tones using pneumatic actuators in quadruped locomotion. In *IEEE Intl. Conf. on Intelligent Robots and Systems* (pp. 2453–2458).

[61] van der Krogt, M., de Graft, W., Farley, C., Moritz, C., Casius, L., & Bobbert, M. (2009). Robust passive dynamics of the musculoskeletal system compensate for unexpected surface changes during human hopping. *J. Appl. Physiol.*, 107, 801–808.

[62] van der Linde, R. (2001). *Bipedal walking with active springs: gait synthesis and prototype design*. PhD thesis, Delft University.

[63] van Ingen Schenau, G., Bobbert, M., & Rozendal, R. (1987). The unique action of bi-articular muscles in complex movements. *J. Anat.*, 155, 1–5.

[64] van Soest, J. & Bobbert, M. (1993). The contribution of muscle properties in the control of explosive movements. *Biol. Cybern.*, 69, 195–204.

[65] Voigt, M., Chelli, F., & Frigo, C. (1998). Changes in the excitability of soleus muscle short latency stretch reflexes during human hopping after 4 weeks of hopping training. *Eur. J. Appl. Physiol.*, 78, 522–532.

[66] Vukobratovic, M. (1972). On the stability of anthropomorphic systems. *Mathematical Biosciences*, 15, 1–37.

[67] Wisse, M. (2004). *Essentials of dynamic walking: Analysis and design of two-legged robots*. PhD thesis, Delft University.

[68] Xie, S. & Jamwal, P. (2011). An iterative fuzzy controller for pneumatic muscle driven rehabilitation robot. *Expert Systems with Applications*, 38, 8128–8137.

[69] Yakovenko, S., Gritsenko, V., & Prochazka, A. (2004). Contribution of stretch reflexes to locomotor control: a modeling study. *Biol. Cybern.*, 90, 146–155.

[70] Yamada, Y., Nishikawa, S., Shida, K., Niiyama, R., & Kuniyoshi, Y. (2011). Neural-body coupling for emergent locomotion: a musculoskeletal quadruped robot with spinobulbar model. In *IEEE Int. Conf. on Intelligent Robots and Systems* (pp. 1499–1506).

Acknowledgments

I would like to thank Professor Koh Hosoda for providing great ideas and advice during my three years in his laboratory. Changing city, university and research theme was difficult, but working with Koh was extremely rewarding. All the support and freedom given through these years helped shaping the results of my research and my life.

Thanks to professors Masahiro Shimizu, Shuhei Ikemoto and Kenichi Narioka, which not only contributed with comments and suggestions to my research, but also personally, being good friends with whom I could speak openly. Special thanks to professor Toru Fujiwara for ”adopting” me in the last 6 months of my PhD, and to professors Shinji Shimojo and Takahiro Hara for reviewing this thesis.

Changing from Hokkaido to Osaka forced me to find new friends, and all the members from Hosoda Laboratory welcomed me with open arms, and I definetely wanted to thank for their kindness. In special, I wanted to thank Shogo Nakatsu and Xiangxiao Liu, which went above and beyond to help me, providing research ideas and performing experiments. I am sure that I wouldn't have reached the same conclusions if it wasn't for their help! I also wanted to thank Miki Yasunaga, which not only helped me with university procedures, but also provided me with sweets to eat while working in the laboratory.

Outside the laboratory environment, I would like to thank Pedro for helping me relax while having drinks, David, Alex and their wives for the many great moments we had, and my fellow foreigners from Osaka University (Omid, Jimmy, Rok, Nina, Martin, Marco, Carla, Haruka and Hussein) for many laughs shared over lunch.

I would also like to thank my two families, one which remains in my country, with my mom, dad and brother, and my new Japanese family, the Shimamura family, which ”adopted” me after living so long away from my country. Thank you guys!

Finally, I wanted to thank my wife and best friend, Mifue Shimamura, whom I dedicate this thesis. I am sure that I wouldn't be here if it wasn't for you.

This thesis approaches legged locomotion from a new angle. Using artificial muscles to recreate animals, it shows that, beyond brain and spinal cord signals, muscle-generated signals also contribute to our locomotion. Through real-world experiments, the stability of hopping and walking biomimetic robots is gauged while they rely on muscles to move in an almost sensorless, open-loop setting. Findings from this work hint to the existence of simple rules coordinating muscle movements, forming the basis of locomotion stability, which brain and spine exploit to produce coordinated movements. A full understandment of such "muscle rules" will not only lead to wider knowledge about animal locomotion, but will ultimately lead to faster, safer and more stable legged robots.